Remote Sensing Applications: Society and Environment 36 (2024) 101321

Contents lists available at ScienceDirect

Remote Sensing Applications: Society and Environment

journal homepage: www.elsevier.com/locate/rsase

Investigation of lineament extraction: Analysis and comparison of digital elevation models in the Ait Semgane region, Morocco

Mohamed Ali EL-Omairi [a], Abdelkader El Garouani [a], Ali Shebl [b, c, *]

[a] Functional Ecology and Environmental Engineering Laboratory, Sidi Mohamed Ben Abdellah University, FST-Fez, P.O. BoX, 2202, Fez, Morocco
[b] Department of Mineralogy and Geology, University of Debrecen, Egyetem ter 1, 4032, Debrecen, Hungary
[c] Department of Geology, Tanta University, Tanta, 31527, Egypt

ARTICLE INFO

Keywords:
Lineaments
DEMs
TPI
Hillshade
Automatic extraction
Structural deformations
Anti-atlas

ABSTRACT

An automated lineament extraction model was successfully applied in the mountainous region of Ait Semgane, Morocco, enabling the identification of geological and tectonic linear features. Our research implemented several approaches including Topographic Position Index (TPI), shading, and Digital Elevation Models (DEMs), as input for the lineament extraction algorithm and applied to various Dems. We aimed to compare all of these strategies to determine the optimal method and the most favorable input DEM. Results revealed variable performance among methods, emphasizing the importance of choosing the optimum method based on specific objectives. TPI and Hillshade methods showed high sensitivity in detecting lineaments, while ALOS PALSAR and Sentinel 1 InSAR datasets were effective for subtle features. Lineament density exhibited specific orientations for highly-dissected zones, with TPI highlighting NE-SW and E-W orientations. Lineament orientations demonstrated consistency with established geology, confirming pre-existing tectonic knowledge. Cartographic analysis of faults emphasized the success of the SRTM DEM model with the TPI method, highlighting significant faults. Results also revealed a concentration of faults in the NW and southern sectors, corroborating bibliographic references and the well-documented tectonic setting of the study area. This automated methodology facilitated lineament extraction in unmapped areas, reinforcing the validity of the undertaken cartographic analysis.

1. Introduction

The Earth's surface configuration is shaped by the combined influence of internal factors such as tectonism and volcanism, along with external processes like weathering and erosion (Jordan et al., 2005; Anbalagan and Singh, 1996). These processes, in conjunction with rock types, existing structures, and the distribution of soils and other surface materials, contribute to the formation of significant geographical and geological features such as faults, folds, and fracture zones (Ramli et al., 2010; Anbalagan, 1992). Among these features are lineaments which may indicate topographical and geological (structural) linear features.

The term "lineament" was first introduced in the early 20th century to describe surface features (Martial et al.; HOBBS, 1904). Over time, this term has evolved, leading to new interpretations and definitions of lineaments (van der Pluijm et al., 2004). According to (O'Leary et al., 1976), lineaments are linear features identifiable on the Earth's surface, characterized by specific patterns of elements arranged in coherent, straight, or slightly curved structures.

* Corresponding author. Department of Mineralogy and Geology, Faculty of Science and Technology, University of Debrecen, Egyetem ter 1, 4032 Debrecen, Hungary.
E-mail addresses: ali.shebl@science.tanta.edu.eg, alishebl@mailbox.unideb.hu (A. Shebl).

https://doi.org/10.1016/j.rsase.2024.101321
Received 30 December 2023; Received in revised form 7 August 2024; Accepted 12 August 2024
Available online 17 August 2024

Over the years, several studies have attempted to extract lineaments using various data and methods, yielding diverse and sometimes contradictory results. The diversity of these methods and the disparities in their results highlight the importance of a rigorous comparative study to determine the optimal method for lineament extraction, especially in specific geographical contexts.

In the field of geosciences, accurate extraction of lineaments is crucial for understanding various geological (Sichugova and Fazilova, 2020), tectonic (Kokinou and Panagiotakis, 2020), and environmental phenomena (Sichugova and Fazilova, 2021) (Sichugova and Fazilova, 2024), whether they have a geological, geomorphological, or artificial nature (Ahmadi and Pekkan, 2021). The use of Digital Elevation Models (DEMs) and detailed lineament analysis is now indispensable for applications such as mineral exploration (Kokinou and Panagiotakis, 2020; Sichugova and Fazilova, 2021; Sichugova and Fazilova, 2024), seismic risk assessment (Moustafa et al., 2022), management of groundwater resources (Es-sabbar et al., 2020; Manuel et al., 2017; Shebl et al., 2021; Moustafa et al., 2022) and engineering constructions (Rahnama and Gloaguen, 2014), providing essential insights into the underlying terrain structure. This approach helps reduce subjectivity and the time required for manual analysis, with widespread applications in other areas of geoscientific research (Takorabt et al., 2018; Magaia et al., 2018). However, the precise identification and mapping of lineaments have long been a significant challenge for researchers and geologists.

Digital Elevation Models are 3D representations of a terrain's surface created from terrain elevation data. They are widely used in geospatial analysis for various applications including lineament extraction. High-resolution DEMs can provide detailed topographic information and are useful for identifying large-scale geological features and terrain characteristics (Zhou, 2017). However, the quality of DEMs can vary depending on the resolution and data source, and processing high-resolution data may require significant computational resources. DEMs have been extensively used in geological studies for mapping terrain features and extracting lineaments.

For this study, we selected four widely recognized Digital Elevation Models in the scientific community: ALOS World 3D, S1 InSAR DEM, ALOS PALSAR, and SRTM. Each of these DEMs offers distinct characteristics that cater to specific needs in terrain analysis. ALOS World 3D, produced by the ALOS satellite, stands out with its high resolution of 5 m (Altinoğlu et al., 2015), allowing for the identification of fine linear features (Cardoso-Fernandes et al., 2022). However, it may exhibit data gaps in densely vegetated or urban areas. The S1 InSAR DEM, utilizing Sentinel-1's interferometric radar technology, provides accurate elevation data ideal for deformation studies, although it requires complex processing (Wu and Lee, 2007). ALOS PALSAR, based on the L-band synthetic aperture radar from the ALOS satellite (Cardoso-Fernandes et al., 2022), offers a 12.5-m resolution and can penetrate vegetation cover, which is advantageous in densely wooded regions. However, it can be affected by atmospheric conditions. The SRTM, produced by the Shuttle Radar Topography Mission, features a 30-m resolution and is widely available, ensuring consistent global coverage (Elmahdy et al., 2021), though it has a lower resolution compared to other sources.

The TPI is a method that compares the elevation of each point on the terrain with the average elevation of neighboring points within a specified radius. It helps in identifying topographic features such as ridges, valleys, and flat areas (Knitter et al., 2019). TPI is effective in distinguishing between different topographic features and provides a detailed analysis of local topography. However, the choice of neighborhood size (kernel size) can significantly affect the results and requires careful calibration to match the terrain characteristics (Bufalini et al., 2021). T

The Hillshade method simulates the illumination of a terrain surface by a light source to create a shaded relief map (Farmakis-Serebryakova and Hurni, 2020). This technique enhances the visualization of terrain features by highlighting slopes, ridges, and valleys. Hillshade analysis is simple to implement using GIS software and helps in identifying linear features that may not be visible in the raw elevation data. However, the effectiveness of the Hillshade method depends on the angle and direction of the simulated light source and may not accurately represent features in areas with complex topography.

These methods were chosen for their ability to provide a detailed and visual understanding of geological and anthropogenic structures in the complex mountainous region of Ait Semgane, and their effectiveness has been validated by previous studies on geomorphological analysis and lineament extraction (Table 1).

The primary objective of this study is to conduct a comprehensive and comparative evaluation of the effectiveness of various DEMs in the lineament extraction process, utilizing remote sensing data and Geographic Information System (GIS) technology (Tang, 2014). We specifically focus on the analysis of four widely adopted digital elevation models in the scientific community: ALOS WORLD 3D (AW3D) with a resolution of 5 m, S1 InSAR DEM with a resolution of 10 m, ALOS PALSAR with a resolution of 12.5 m, and SRTM from ASTER with a resolution of 30 m. To achieve this, we employ three distinct methods: direct extraction from DEMs (Bourjila et al., 2021; Rahnama and Gloaguen, 2014), the TPI method (Šilhavý et al., 2016; Lu and An, 1999) and the Hillshade method (Zhou, 2017; Altinoğlu et al., 2015). These data are complemented by in-depth statistical analysis and precise photogeological interpretation. This comprehensive process aims to gain insights into the spatial concentration and orientation of lineaments in the study area, paving the way for significant advances in geological mapping and modeling complex terrestrial phenomena. The thorough comparison seeks to provide researchers and professionals with guidance on the optimal selection of DEM based on the specific needs of their study area.

2. Geomorphological and geological parameters

2.1. Geographic location

The study area, depicted on the 1/50,000 geological map of Aït Semgane, is situated southeast of Ouarzazate in the Zagora province, Tansifte commune, Morocco (Fig. 1). Geographically, it is part of the southern section of the Central Anti-Atlas. The coordinates of the area range between latitudes 31°30'N and 31°45'N and longitudes 6°30'W and 6°45'W. The area exhibits diverse relief types influenced by climatic, lithological, and tectonic factors.

Table 1
Comparison of results from studies related to lineament extraction using various techniques and data.

Reference	Used data	Method	Results
Yun and Moon (2001)	DEM produced at 1:50,000 scale with a sampling interval of 1 arc second (approximately 30 by 30 m)	Drainage network	The method employed terrain slope analysis and a hierarchical Hough transform. The results illustrated that the method successfully extracted linear features, providing valuable information for geological interpretation.
Villalta Echeverria et al. (2022)	ALOS PALSAR DEM (12.5m)	TPI	The study identified 76 geological lineaments, including faults, anticlines, and synclines. The lineaments exhibited a preferential NE-SW orientation and an important family of NW-SE orientations. The methodology presented in the study can optimize time and reduce costs in gathering structural information for geological and mining prospecting.
Abdullah et al. (2010)	SRTM DEM	Slope image created from digital elevation models	The results show a positive correlation between the extracted lineaments and the geological structures of the region. The data used includes a DEM, topographic maps and field observations.
Abdelkareem et al. (2020)	Landsat-8/Sentinel-1/ALOS/PALSAR/ACP/MNF	Simple extraction (using PCI Geomatics LINE tool for automated extraction)	The use of Sentinel-1 and SRTM digital elevation models has provided enhanced terrain perspectives. The results have highlighted dominant linear features, including north-south foliations associated with tight folds and major strike-slip faults
Shebl and Csámer (2021)	Landsat OLI, ASTER, Earth Observing-1 Advanced Land Imager, Sentinel 2A, Sentinel 1, ALOS PALSAR, SRTM, NASA, ASTER V3	The lineaments extraction was accomplished by integrating edge detection and line linking algorithms	The results indicate that optical sensors used are less effective than DEMs with the same spatial resolution. Sentinel-1 radar data outperforms optical data sources. The ALOS PALSAR DEM (12.5m) is more suitable than any other type of data used, including Sentinel-1 data (10 m)
Javhar et al. (2019)	Landsat-8, Sentinel-2A, Sentinel-1A	Automated approach	Sentinel-1A radar images demonstrated the highest correlation among automatically extracted lineaments, manual interpretation, and the existing map of lineaments. Radar data enabled the extraction of 5872 and 5865 lineaments for VH and VV polarizations respectively, whereas Landsat-8 and Sentinel-2A optical data extracted 2338 and 4745 lineaments respectively.
Ahmadi and Pekkan (2021)	TM, ETM+, OLI/TIRS, ASTER et Sentinel 2, Sentinel 1, InSAR, ALOS PALSAR	Manual and automated techniques	The review highlights the importance of remote sensing techniques in identifying geological lineaments and underscores the necessity of integrating both manual and automated approaches to achieve accurate results
Ghosh et al. (2021)	SAR data	Lineament extraction module (LINE) in PCI Geomatics software	The SAR sensor parameters, such as frequency, polarization, and viewing angle, play a crucial role in enhancing performance for a specific application. The study also analyzes the spatial distribution of lineaments concerning the local structural regime, thus providing a better understanding of the regional tectonic configuration.
Soliman and Han (2019)	SRTM V3	Manual techniques (based on visual interpretation) and automated techniques	The study demonstrates the importance of vertical accuracy in DEMs for the accuracy of lineament extraction. The appropriate choice of DEM can significantly enhance the quality of extraction results. This underscores the importance of accurate evaluation of DEMs in remote sensing-based geological applications
Hashim et al. (2013)	ASTER GDEM/Landsat-8 OLI B5	Wavelet transform	The article achieves a precise match with major faults such as Kuangshanchang Fault, Dongtou Fault, and Niulan River Fault.
Rauf et al. (2023)	DEMNAS	Automated approach	The article provides a comprehensive analysis of geothermal lineaments in a geologically complex region, demonstrating its practical applicability in the field of geothermal exploration. The predominant structure exhibited a northeast-southwest (NE-SW) and northwest-southeast (NW-SE) orientation.
Tende et al. (2022)	Aster DEM	Manual and automated approach techniques	The study introduces an innovative hybrid methodology combining both automatic and manual extraction of lineaments. This hybrid approach provides a solution to the challenges associated with lineament extraction by combining the speed of automation with the accuracy of manual extraction.
Ahmadi and Pekkan (2021)	Landsat, ASTER, Sentinel 2, SRTM DEM, SAR, InSAR, Sentinel 1	Manual, semi-automated, and automated	This paper provides a systematic review of remote sensing techniques and data sets used for the analysis of geological lineaments, which are important features related to tectonic activity, minerals, faults, groundwater, earthquakes, and geomorphology.
Kokinou and Panagiotakis (2020)	Slope and aspect images and their derivatives	Combine slope and aspect images to compute an enhancement image F that highlights seafloor texture and lineaments	The proposed method of multiple filtering and skeletonization can accurately extract tectonic lineaments and seafloor features related to evaporite movements, even with limited ground truth data. The accuracy of the lineament extraction depends on the quality of the bathymetric data (DEM). Robust criteria like detection strength, length, direction, and spatial distribution of the lineaments can be used to interpret the bathymetric patterns and distinguish between tectonic and evaporite-related features.

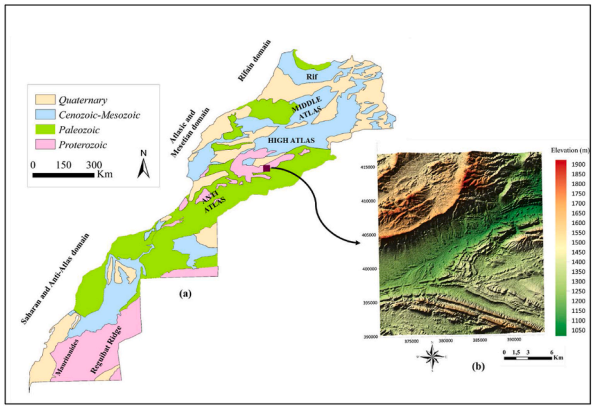

Fig. 1. (a) Geographic location of the study area & (b) Digital elevation model S1InSaAR of the study area.

This region was chosen for the study due to several compelling reasons. Firstly, the Central Anti-Atlas is known for its complex geological structure, making it an excellent case study for analyzing lineaments and understanding their formation and distribution. The area is characterized by significant tectonic activity, which has resulted in a variety of geological features that are ideal for anthropogenic linear objects. Furthermore, the presence of diverse lithological units provides an opportunity to examine the influence of different rock types on lineament formation. Additionally, the region's accessibility and existing geological data, such as the 1/50,000 geological map, facilitate detailed fieldwork and data validation. Importantly, this area has not been the subject of a similar comprehensive study before, making it a novel site for investigating the spatial distribution and characteristics of lineaments. Studying this area can provide valuable insights into the geological evolution of the Anti-Atlas and contribute to broader geospatial and geotectonic research.

2.2. Geomorphology

According to the comprehensive study of the Saghro's geomorphology and its impact on the Saharan region conducted by (Riser, 1988), the study area exhibits a remarkable configuration. It comprises a high mountain range, acting as a veritable water tower on the edge of the desert and playing a crucial role in the Pleistocene evolution of surrounding valleys and plains. The central part of the region is predominantly composed of resilient granites and volcanic rocks, with peaks surpassing 1800 m in altitude (Riser, 1988) (Fig. 2). Other geological formations, less resistant such as sedimentary or magmatic rocks, have eroded to form extensive mountain plains situated between 1300 and 1500 m in altitude (Abdelkareem et al., 2020). The alternation of hard and soft geological layers has been instrumental in shaping the observed morphological structures.

The climatic variations have played a predominant role in the morphological evolution and diversity of geomorphological features in the region (Walsh et al., 2012). Their variety and complexity are attributed to the proximity of the Saghro to the Sahara. The hydro-

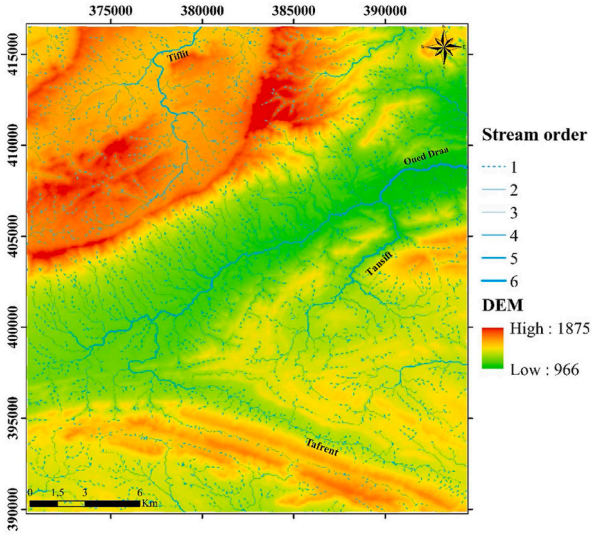

Fig. 2. Map of the hydrographic network in the study area.

graphic network of the study area is highly developed, with a preferential north-south and east-west orientation, as illustrated in Fig. 2.

The Draa and Tansift rivers are among the most important, while the tributary Assifs of the Draa are among the least significant (Bajja, 1987).

The climate in the area is arid, as highlighted by (Riser, 1988) and (Agoussine et al.). The vegetation is characterized by the presence of thorny acacias, jujubes, oleanders, and palm trees near water points (Batchelor and Bowden, 1985). Clumps of wormwood, lavender, and other plants are also found, providing pasture for the numerous sedentary and nomadic animals in the region (Batchelor and Bowden, 1985).

2.3. Geological context

The Anti-Atlas, located on the northern edge of the West African Craton, has been the site of Eburnean, Pan-African, and Hercynian orogenies that occurred in chronological order during the Palaeoproterozoic, Neoproterozoic, and Paleozoic eras, respectively, shaping successive crowns along the Craton's edge and thus expanding it (Leblanc, 1975).

In the Proterozoic era, formations from the Middle and Upper Neoproterozoic (NP2i, NP2s, NP3i, and NP3s) are well-represented in the region (Emran and Chorowicz, 1992). These formations encompass a variety of rocks such as volcanic rocks, granite intrusions, conglomerates, sandstones, siltites, and shales (Fig. 3) (Leblanc and Lancelot, 2011). Major unconformities separate these sets, marking key phases in the geological evolution of the region.

In the Paleozoic era, the post-Ediacaran cover predominates, occupying the majority of the Aït Semgane region. This cover is composed of conglomerates, sandstones, siltstones, dolomites, and basalts, representing the Cambrian and lower Ordovician epochs (Fig. 3). These formations bear witness to a succession of sedimentary strata characteristic of the Paleozoic era (G and Choubert, 1986).

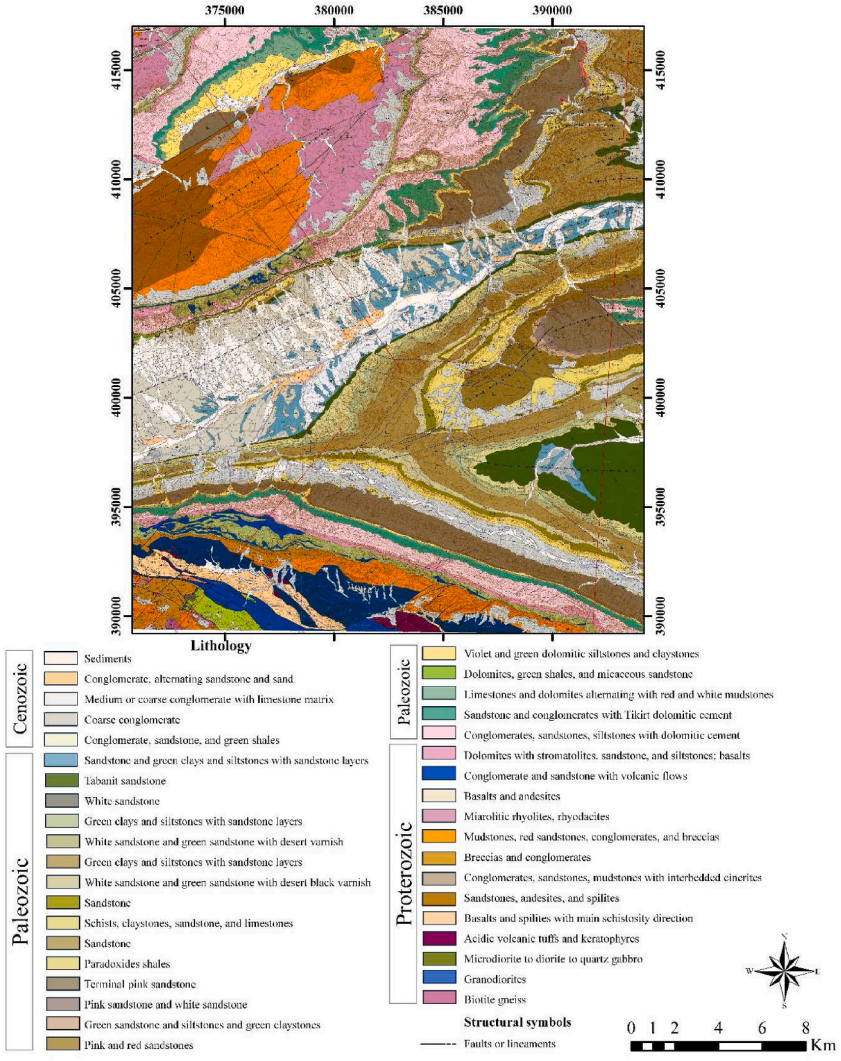

Fig. 3. Geological map of the study area, based on Yazidi et al. (Yazidi et al., 2008).

In the Quaternary, the region has been marked by cycles of erosion and fluvial deposits in response to climatic changes (Görler et al. Jacobshagen, 1988). Quaternary deposits (alluvium and conglomerate) include terraces and alluvial fans formed during glacial and interglacial periods (Nahid, 2001). These cycles are linked to climatic variations, with phases of intense erosion during rainy periods, followed by gravel and sand deposits by rivers (Görler et al. Jacobshagen, 1988).

2.3.1. *Structural context*

Numerous faults cut across the terrains in the area. The oldest faults run along the edge of the NP2i formations in the Bou Azzer-El Graara graben. This fault zone corresponds to the major fault of the Anti-Atlas (Fig. 4), separating the West African craton and its continental margin to the south from a volcanic arc to the north (Riser, 1988; Batchelor and Bowden, 1985; Leblanc, 1975).

The major deformation in the region occurred during the PA2 event, with vertical to steeply south-dipping faults and lineation indicating dominant NE-SW-directed thrusting (Hefferan et al., 2000).

The metabasalts and serpentines are strongly foliated in the major fault zone of the Anti-Atlas fault in the area, and the most visible lineations dip slightly to the west. The entire area exhibits a dominant overlap with a main stress direction of NE-SW during PA2 (D'Lemos et al., 2006).

In the cover, the Hercynian E-W folds and faults are generally consistent with the rotation of the stress field, possibly inheriting the direction of the ancient Pan-African faults (Görler et al. Jacobshagen, 1988). Some faults in the cover show normal or sinistral movements, reflecting the reactivation of antithetic PA3 faults in the basement (Admou, 2011).

3. Materials and methods

In the context of this study, a precise methodology was employed to optimize the extraction of lineaments from different sources of DEMs. Data were acquired from ALOS World 3D (5m), S1 InSAR DEM (10m), ALOS PALSAR (12.5m), and SRTM (30m). After preprocessing, including the creation of TPI and hillshade models, the automatic extraction of lineaments was performed using the line module of PCI Geomatica 2018. The extracted lineaments underwent visual inspection, filtering, and in-depth analysis using Google Earth. This approach aimed to exclude lineaments that did not correspond to specific geological features, such as rivers or layer boundaries. Fig. 5 illustrates the overall flowchart of the procedure executed in this study.

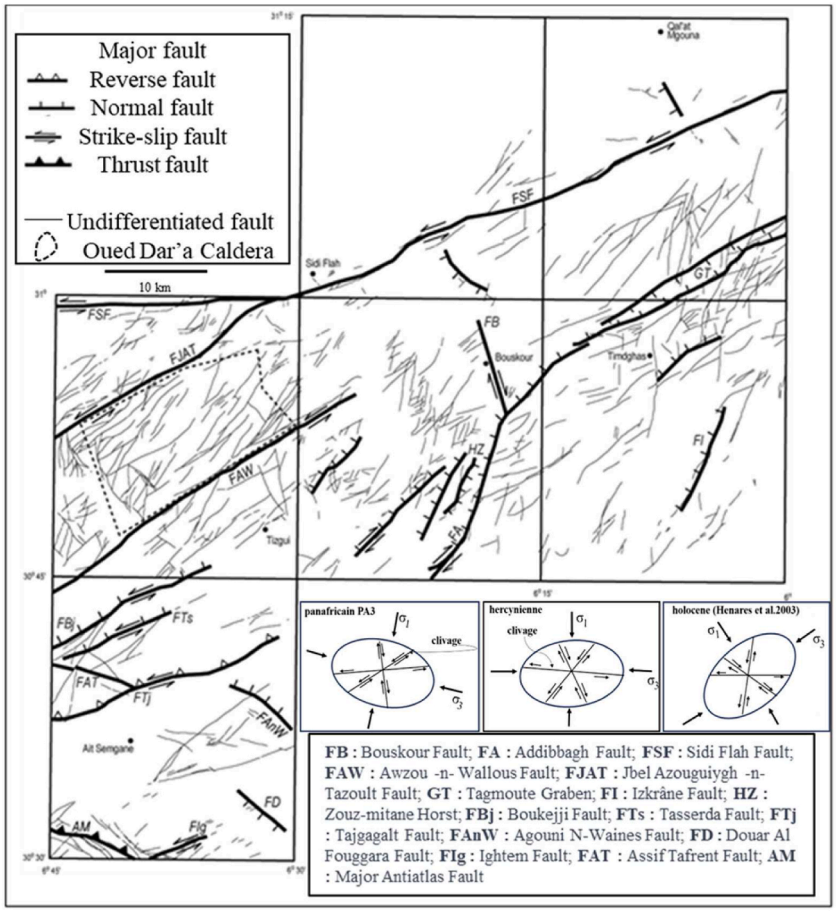

Fig. 4. Map of major faults in the study area (Yazidi et al., 2008).

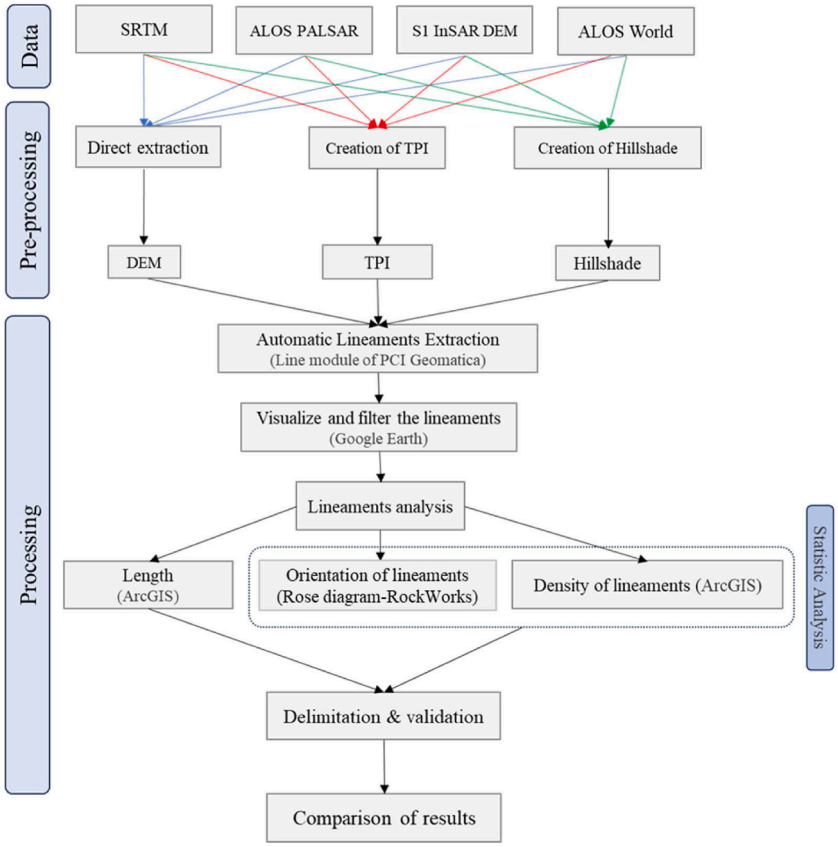

Fig. 5. Methodology employed in this study.

3.1. Data acquisition

The data utilized in this study encompass DEMs from diverse sources, each possessing specific resolutions tailored to meet the analysis requirements.

Precise topographic details were derived from the high-resolution ALOS World 3D data, offering an intricate view of the study terrain. S1 InSAR DEM provided a broader perspective while retaining ample resolution to identify crucial features. ALOS PALSAR complemented the analysis by offering an intermediate view between finer resolutions, ensuring a comprehensive understanding of the terrain.

To contextualize topographic features on a broader scale, SRTM data was integrated. Despite a slightly lower resolution, these data played a crucial role in obtaining an overarching view of the terrain, facilitating a comprehensive analysis of lineaments within their global context.

3.2. Data preprocessing

The meticulous preparation of raw data was a crucial step in the methodology, ensuring accurate and reliable results in the analysis of lineaments. To begin, the data underwent a thorough examination and correction process to eliminate potential errors and ensure consistency. This procedure enabled the detection and rectification of possible inconsistencies, such as sensor artifacts, outliers, and topographic anomalies, thereby ensuring the reliability of the information used in our geological analysis.

The digital elevation models was analyzed using the TPI and the Hillshade method. The TPI was computed for each specific point on the terrain. This method involves comparing the elevation of each point with the average elevation of neighboring points within a certain radius (Fig. 6) (Görler et al. Jacobshagen, 1988; Nahid, 2001).

By calculating this ratio, we were able to identify precise topographic variations at each location, distinguishing between ridges and valleys and thus revealing subtle details of local topography. Positive TPI values indicate elevations higher than the local average, while negative values indicate depressions or lowlands (Knitter et al., 2019), allowing for a detailed analysis of terrain features at the local scale.

This index is computed in ArcGIS using the ***"Focal Statistics"*** tool, which calculates the local average elevations in a defined neighborhood around each point in the DEM. This local average served as a reference for each location, enabling us to understand specific topographic variations at each point.

Next, the ***"Minus"*** tool was used to subtract the original DEM from the raster representing the calculated local average. This operation resulted in the creation of the TPI, highlighting local topographic fluctuations, ranging from ridges to valleys.

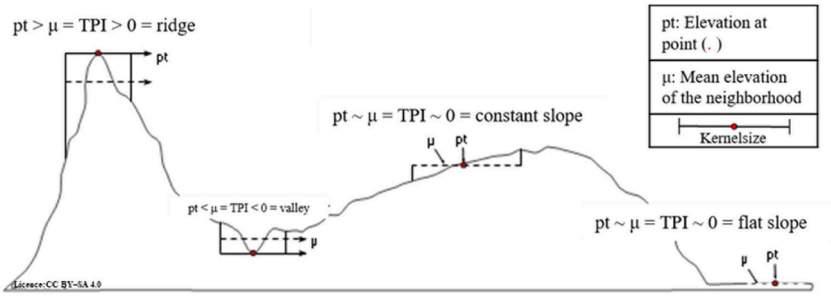

Fig. 6. Principle of the TPI, based on Knitter et al. (Knitter et al., 2019).

The window size, or kernel size, is a critical parameter in TPI analysis as it defines the neighborhood over which the local average elevation is calculated (De Reu et al., 2013). In this study, the choice of window size was based on a balance between capturing meaningful topographic features and avoiding excessive smoothing of the terrain. Given the different resolutions of the DEMs used in this study (ALOS WORLD 3D at 5 m, S1 InSAR DEM at 10 m, ALOS PALSAR at 12.5 m, and SRTM at 30 m), the kernel size was adjusted to reflect the scale and resolution of each dataset. Specifically, we used a larger kernel size for lower resolution DEMs to ensure that significant topographic features were captured adequately, while a smaller kernel size was applied to higher resolution DEMs to avoid oversmoothing and to retain detailed local variations.

The resolution of the DEM significantly affects the outcome of the TPI analysis. Higher resolution DEMs provide more detailed and accurate representations of the terrain, allowing for the identification of finer topographic features (Wu et al., 2008). However, they also require a smaller kernel size to prevent the loss of detail. Conversely, lower resolution DEMs tend to generalize the terrain features, necessitating a larger kernel size to capture broader topographic patterns effectively.

In mountainous terrains, such as the study area, this adjustment is particularly important. A carefully chosen kernel size ensures that both major landforms and minor features are appropriately represented in the TPI analysis. The results obtained from different DEMs were compared to assess the consistency and reliability of the extracted lineaments, considering the inherent resolution and topographic complexity of each dataset.

Simultaneously, the Hillshade model was generated to create striking visual representations of the terrain. By simulating the angle and intensity of sunlight, these models produced realistic shadow and light effects on the relief (Najafifar et al., 2019) (Fig. 7).

The details such as ridges, aspects (Fig. 8), and slopes (Fig. 9) have been clearly defined, making it easier to visually identify important topographic features. This dynamic visualization has been crucial for discerning subtle variations in the terrain, aiding in the identification of potential lineaments.

Area's exposure refers to the orientation of the terrain surface in relation to the cardinal directions (north, south, east, west). It is an important topographic feature because it influences the amount of sunlight and wind a specific area receives, which in turn affects vegetation growth, soil moisture, and erosion patterns. In geomorphological studies, understanding the exposure of different areas helps in analyzing how these environmental factors influence the development and distribution of landforms and geological structures.

Aspect is a specific component of area's exposure and refers to the direction a slope faces. It is typically measured in degrees, with 0° representing north, 90° east, 180° south, and 270° west. Aspect maps, such as the one shown in Fig. 9, visually represent the direction of slopes across the study area. By analyzing aspect, researchers can gain insights into the geomorphological processes at work, such as the influence of prevailing winds and the direction of water flow, which are critical for identifying and understanding the distribution of lineaments and other geological features.

These preliminary steps have laid a solid foundation for our subsequent analysis of lineaments, ensuring the quality of the results obtained (Fig. 10).

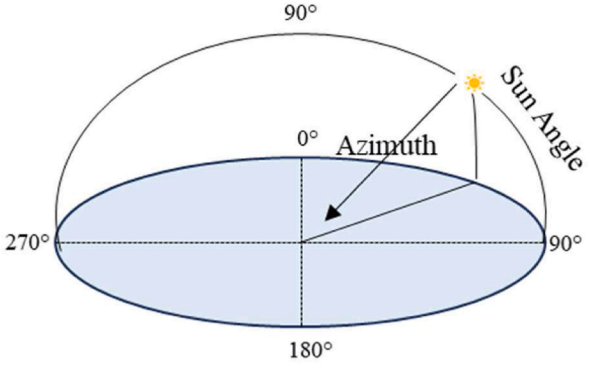

Fig. 7. Principle of the Hillshade model (modified from (Horn, 1981)).

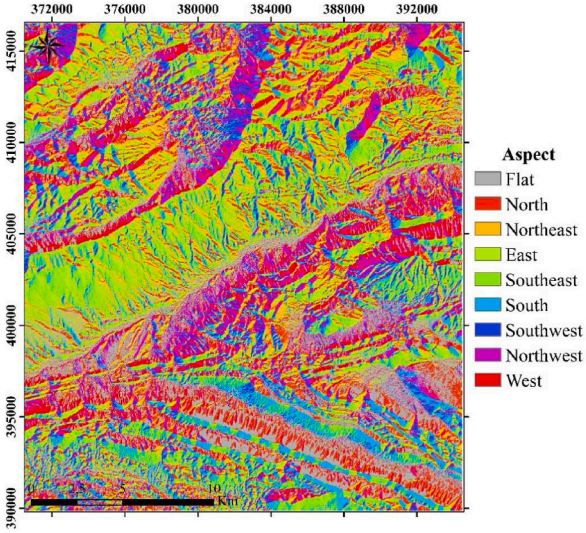

Fig. 8. Map of the study area's exposure.

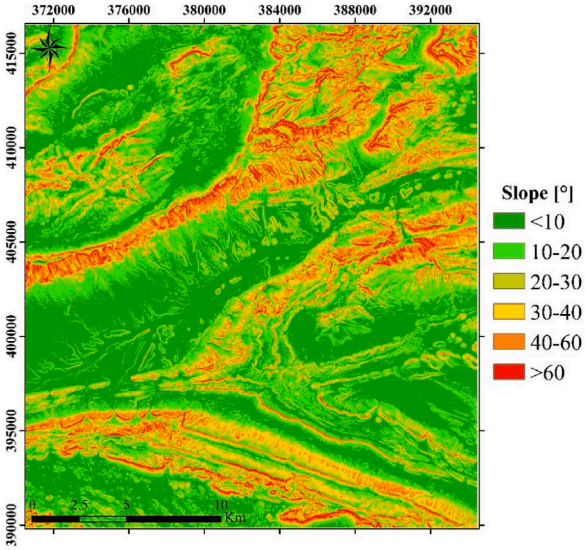

Fig. 9. Map of the study area's slopes.

3.3. Data processing

In the realm of geospatial analysis, precise extraction of linear features is essential for understanding the geological and topographical characteristics of the terrain. PCI Geomatica, one of the most sophisticated and versatile software in the field, offers a powerful and specialized tool for this crucial task: the LINE Module (Lineament Extraction). This module relies on cutting-edge algorithms, combining edge detection and curve extraction techniques to accurately identify discontinuities and linear structures in geospatial data (El-Naqa et al., 2010).

One key feature of the LINE Module lies in its flexibility. It provides a diverse range of customizable parameters, allowing users to finely adjust detection thresholds, minimum lineament lengths, and other essential criteria. This ensures precise adaptation to various geological and topographical conditions, maximizing the accuracy of results (Salui, 2018).

The LINE Module also stands out for its intelligent multi-stage approach. It begins by applying the Canny edge detection filter, an algorithm renowned for its robustness and precision (Salui, 2018). Subsequently, curves are extracted from the detected edges, and these curves are transformed into lineaments through meticulous adjustment of line segments. This meticulous process ensures reliable results, even in areas where linear features are subtle or complex. Key parameters significantly influencing edge detection and curve extraction are carefully selected to guarantee reliable and accurate results (Fig. 11).

The parameter values were chosen after careful testing and iterations to ensure accurate detection of lineaments. The filter radius was set to 5 pixels, a value small enough to capture fine details of the lineaments without introducing too much noise. This choice was

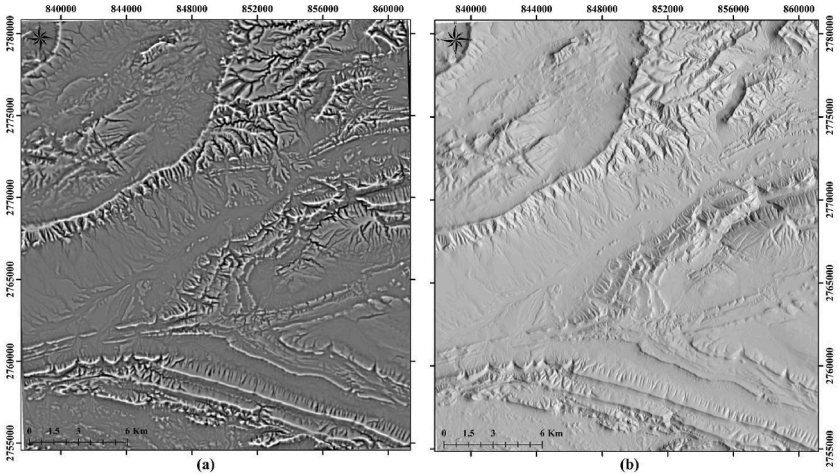

Fig. 10. TPI model (a) and Hillshade model with an azimuth of 90 from S1 InSAR DEM (b).

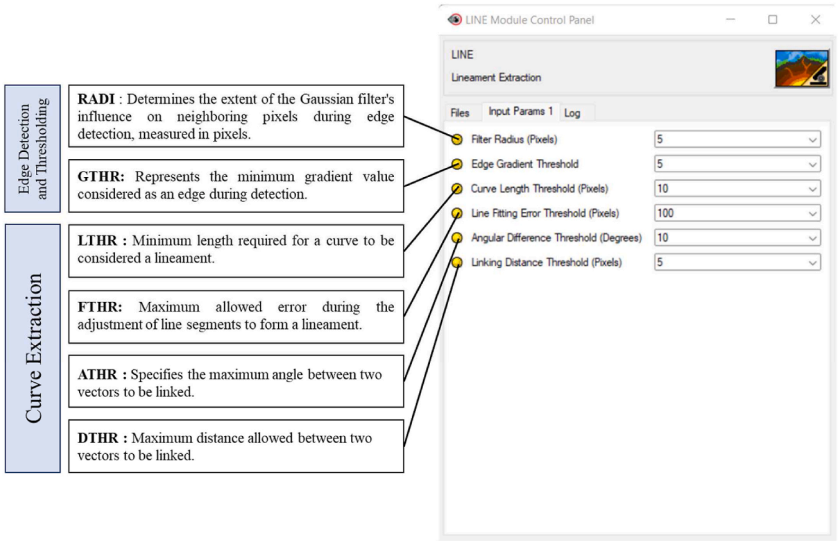

Fig. 11. LINE module parameters in Geomatica software.

made after testing smaller and larger values, finding that 5 pixels offered a good balance between noise reduction and detail preservation.

The edge gradient threshold was set to 5. This threshold was chosen to detect significant changes in the image gradient, which are crucial for identifying lineament edges. A value of 5 was deemed optimal after several manual adjustment iterations, as lower values detected too much noise, while higher values missed important lineaments.

The curve length threshold was set to 10 pixels, determining the minimum length of detected curves. This value ensures that only significant curves are extracted, eliminating small artifacts. Lower values included segments too short to be relevant, while higher values omitted potentially important lineaments.

The line fitting error threshold was set to 100 pixels. This threshold allows for some tolerance in the line fitting process, capturing lineaments with flexibility without being too strict. Stricter values led to the elimination of real lineaments, while more tolerant values included too much noise.

The angular difference threshold was set to 10°, controlling the acceptable angular difference for connecting line segments. This value allows for some flexibility while maintaining accuracy. Smaller values limited segment connection, and larger values increased connection errors.

Finally, the linking distance threshold was set to 5 pixels, determining the maximum distance for connecting line segments. This value connects nearby segments without linking unrelated segments. Larger values connected unrelated segments, while smaller values failed to connect relevant nearby segments.

To ensure consistency and allow for direct comparison of results, the same parameter values were used for all approaches in this study. This approach guarantees that any observed variations in the results are attributable to differences in the methodologies themselves rather than the chosen parameters.

3.4. Post-processing

3.4.1. Visualization and filtration of lineaments

In the methodology, the step of visualizing and filtering lineaments is orchestrated with a high level of expertise, fully leveraging the advanced capabilities of Google Earth. Through Google Earth, we have access to detailed three-dimensional observation of the terrain, providing a complete immersion into the extracted lineaments. This immersive visualization facilitates an in-depth exploration of linear features, highlighting the subtleties of their spatial arrangement. It has allowed us to examine each lineament from various angles and perspectives, enriching the understanding of complex geological structures.

The filtering of lineaments is a crucial step aimed at refining the selection. By applying rigorous criteria such as length, orientation, and relationships with other geological formations, we selectively filter lineaments to retain only the most relevant features. This meticulous approach ensures that only geologically significant lineaments are preserved, eliminating background noise and irrelevant elements (Fig. 12). This rigorous process enables us to obtain precise and reliable data, essential for our in-depth analysis of geological structures in the study area.

3.4.2. Lineament analysis

Quantitative and qualitative methods were employed to analyze the lineaments. In the quantitative aspect, a statistical analysis was conducted, focusing on the number, length, and density of lineaments. These analyses were performed using ArcGIS 10.8.2 software, involving detailed calculations and processes. This rigorous approach allowed us to obtain precise and reliable data, serving as the basis for the in-depth study of linear features in the study area.

3.4.3. Lineaments orientation

The orientation of lineaments is a crucial aspect of our study. By analyzing their general direction, we can discern significant trends in the landscape, revealing patterns that may be related to geological, tectonic, or even environmental phenomena. This analysis enables us to interpret the geological history of the region, shedding light on the forces and processes that contributed to the formation of observed lineaments.

3.4.4. Lineaments density

The analysis of lineament density is a valuable method to assess the intensity of lineaments in the study area. By calculating the density of lineaments, we can identify areas with a higher concentration of linear features. This allows us to delineate key areas where lineaments are most pronounced, providing valuable insights for understanding regional geology. Additionally, this analysis helps assess the potential impact of lineaments on various environmental aspects, such as hydrology and soil erosion, contributing to effective and sustainable land planning.

By combining lineament orientation with the analysis of their density, our study offers an in-depth view of linear features in the region, allowing for a rich contextual interpretation for various geo-scientific and environmental applications.

3.4.5. Delimitation and validation

Once we obtained the lineament density, we used the density map along with the identified lineaments of interest as reference points to delineate the main linear features in the study area. Lineaments, as clearly defined linear features in the terrain, contain crucial information across various domains beyond the geological sphere. These elements can reveal trends, patterns, and structures in

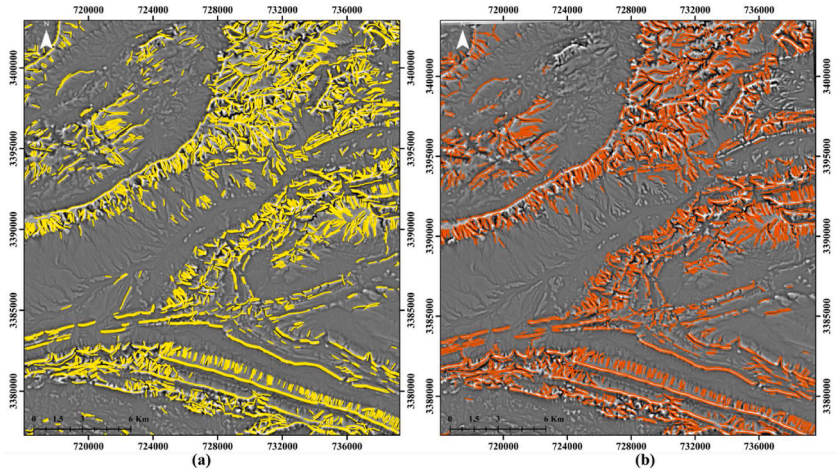

Fig. 12. Lineaments automatically extracted from the S1 InSAR DEM using the TPI method (a), lineaments after filtering (b).

the natural landscape, influencing various environmental and human processes. This methodology allowed for the exploration of relevant lineaments while excluding those that were less pertinent or false lineaments, ensuring a precise and meaningful selection of linear features in our study.

Photo-interpretation played an essential role in refining the understanding of lineaments by enabling the identification of subtle details and visually validating the extracted faults. The analysis focused on geomorphological features, variations in color and texture, as well as linear patterns on Google Earth images to confirm the lineaments determined by the analytical methodology. A crucial validation step in the field involved meticulously planned missions during the month of October 2023. These missions aimed to measure and verify the extracted faults according to the previously described methodology.

4. Results

4.1. Comparative analysis of lineaments

The features extracted directly from various DEMs (Fig. 13), using the Hillshade method (Fig. 14), and TPI method (Fig. 15) underwent a comparative analysis to determine the optimal method and the most suitable DEM for lineament extraction in the study area. Regarding the shading method, several directions were explored (N45, N90, N135, and N315), but it was observed that the N90 direction offered the best identification of lineaments for the N-S direction. According to the literature, the region is characterized by an abundance of NE-SW and E-W oriented faults (D'Lemos et al., 2006; Admou, 2011; De Reu et al., 2013). The lineaments were extracted from these DEMs by applying the same parameters used in the LINE module.

These results highlight the diversity in the performance of analysis methods, underscoring the importance of a strategic approach in selecting the method and dataset based on the specific objectives of the geospatial study. When examining the number of detected lineaments (Fig. 16), the TPI and Hillshade methods prove to be particularly sensitive, providing a detailed perspective on linear features in the terrain. This increased sensitivity can be crucial in contexts such as detecting geological fractures or natural linear structures. On the other hand, the abundance of lineaments extracted from the ALOS PALSAR and S1 InSAR datasets suggests an enhanced ability to identify subtle linear features, which can be particularly useful in detailed geomorphological analyses.

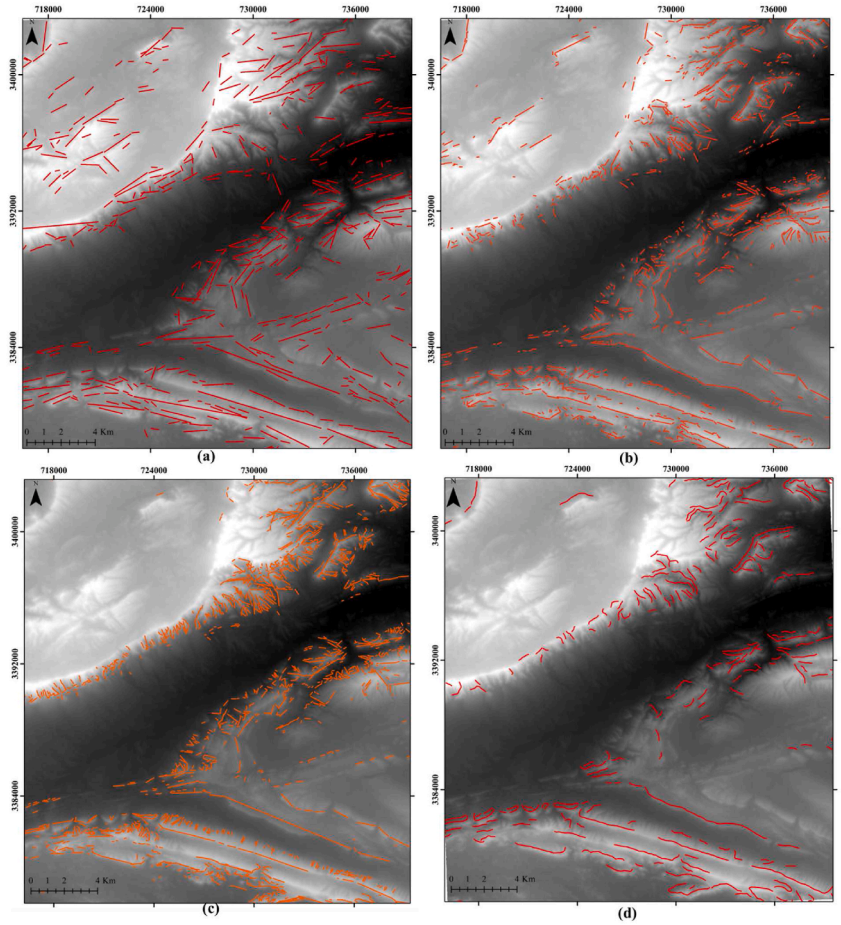

Fig. 13. Comparison of results from automatic extraction using various DEMs: SRTM (a), ALOS PALSAR (b), S1 InSAR (c), ALOS WORLD (d).

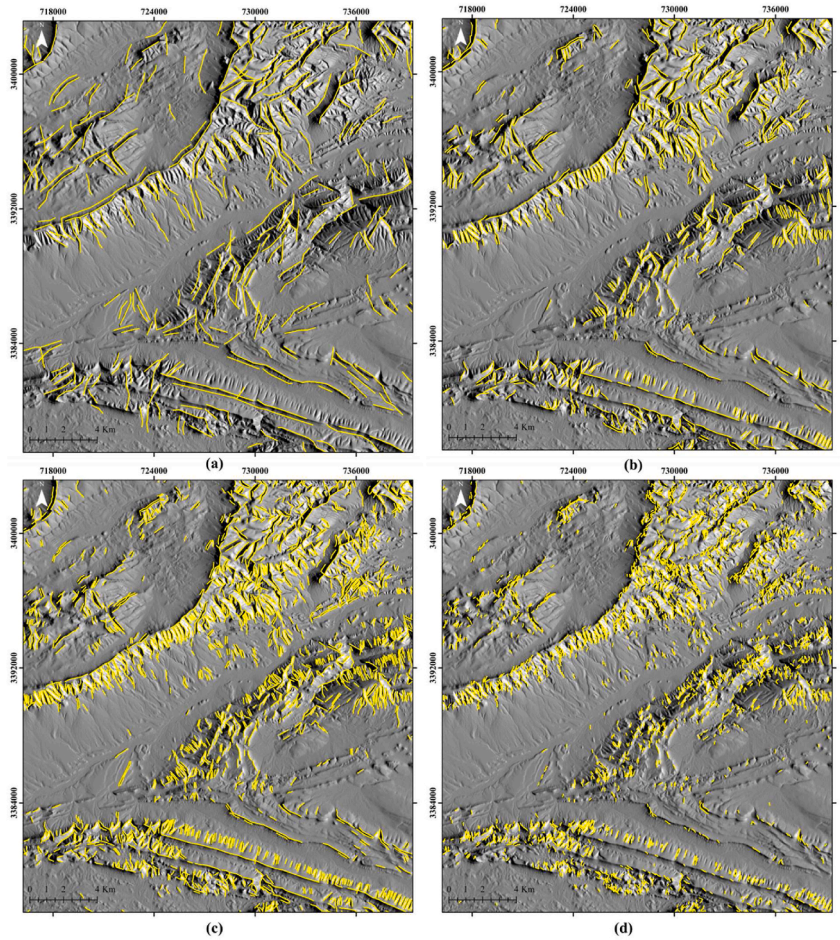

Fig. 14. Comparison of results from automatic extraction using the Hillshade method: SRTM (a), ALOS PALSAR (b), S1 InSAR (c), ALOS WORLD (d).

The variation in the lengths of lineaments between methods and datasets raises important considerations (Table 2). Lineaments extracted from the TPI and Hillshade methods appear to be shorter on average, which may reflect increased sensitivity to small to medium-scale linear features. Additionally, the ALOS WORLD and ALOS PALSAR datasets exhibit generally shorter lineaments, suggesting an ability to detect finer linear structures or landscape elements with higher spatial resolution.

The very high number of lineaments shown by the TPI on ALOS WORLD (Fig. 17) can be attributed to several factors. Firstly, the ALOS WORLD data has a higher resolution, which allows for capturing more detailed topographic features compared to DEM data. This increased resolution enables the TPI to detect finer variations in the terrain, leading to the identification of more lineaments. Additionally, the TPI method is highly sensitive to changes in elevation, making it capable of detecting subtle differences in the topography that might be overlooked by other methods. Consequently, this sensitivity results in a higher number of detected lineaments when using high-resolution data like ALOS WORLD.

On the other hand, the TPI method stands out for detecting a high number of lineaments, while the Hillshade method shows particular sensitivity to small-sized linear features. The specificity of ALOS WORLD, with small-sized lineaments for all three methods, adds an additional dimension to the understanding of topographic features in this geospatial study. The choice between the three methods remains determined by the specific objectives of the study, emphasizing the importance of considering the nature of the topographic features being sought.

It is important to note that the outcome obtained when applying the LINE module of PCI Geomatics is intrinsically linked to the values assigned to the six specific parameters of this module. These parameters, in turn, are closely dependent on the characteristics specific to the studied area, the defined objectives for the study, as well as the resolution of the employed data.

4.2. Analysis of lineament length

A comprehensive analysis of the results highlights distinct trends in the detection of lineaments based on their length, utilizing the TPI and Hillshade methods, as well as those directly extracted from various Digital Elevation Models (DEMs) (Fig. 17).

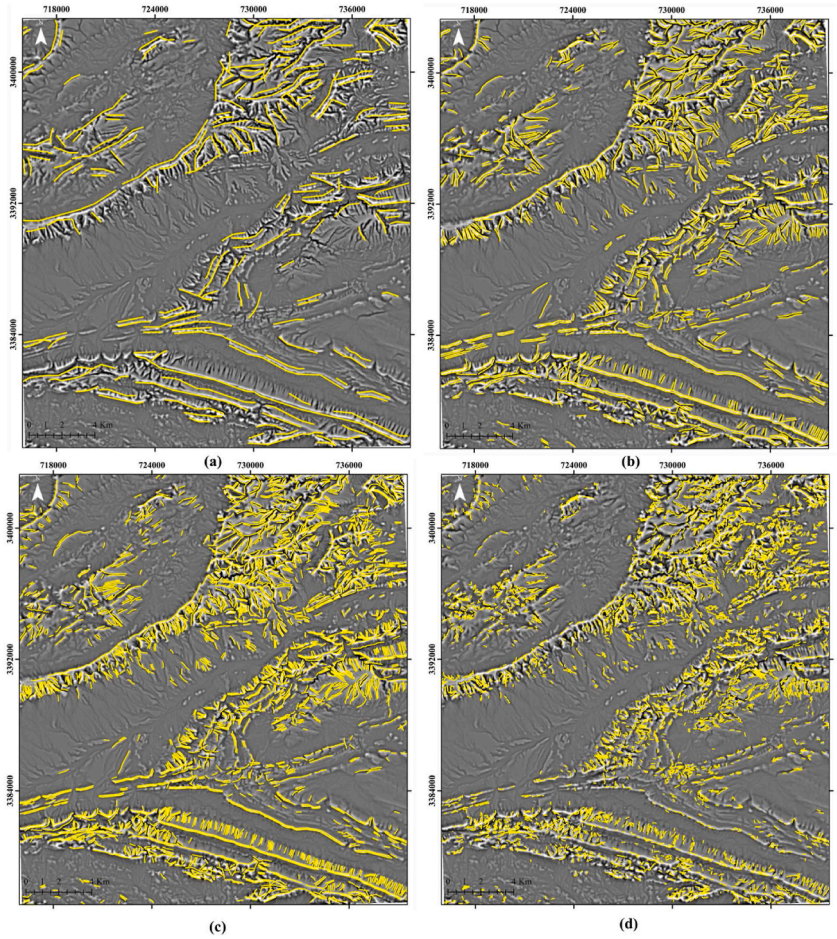

Fig. 15. Comparison of results from automatic extraction using the TPI method: SRTM (a), ALOS PALSAR (b), S1 InSAR (c), ALOS WORLD (d).

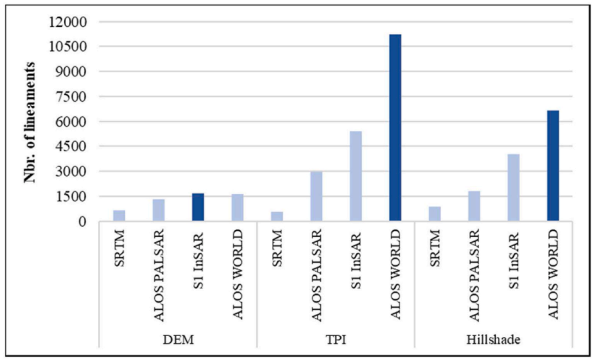

Fig. 16. Histogram showing the number of lineaments extracted from different DEMs using the DEM, TPI, and Hillshade approaches.

In the length range of 0–200 m, the ALOS WORLD DEM (Fig. 18b and c) stands out with a notably high number of 10,828 and 6352 lineaments, demonstrating a particular ability to detect small-sized topographic features. In contrast, the DEM method shows significantly lower figures in this range, with a slight superiority of the S1 InSAR DEM.

For lineaments in the range of 200–400 m, the TPI method based on S1 InSAR DEM (Fig. 18 b) takes the lead with 1955 detected lineaments, surpassing other methods and highlighting increased efficiency in detecting medium-sized topographic features. The range of 400–600 m shows a relatively similar distribution among methods, although the TPI method based on ALOS PALSAR DEM maintains a slight predominance. In the categories of 600–1000 m and 1000–2000 m, all three methods, based on different DEM sources, show comparable performance, demonstrating their competence in detecting lineaments of these lengths. However, beyond 2000 m, the lineament length categories show more modest results, with limited numbers of detected lineaments.

Table 2
Statistics related to lineaments extracted from various methods and DEMs.

Method	Dem				TPI				Hillshade			
Data	SRTM	ALOS PALSAR	S1 InSAR	ALOS WORLD	SRTM	ALOS PALSAR	S1 InSAR	ALOS WORLD	SRTM	ALOS PALSAR	S1 InSAR	ALOS WORLD
Min. length (m)	43,22	25,01	17,23	16,50	59,57	3,16	17,22	8,21	53,28	24,99	17,22	8,21
Max. length (m)	8360,25	2352,44	8119,83	3296,70	3638,01	2635,94	1606,96	636,02	3779,89	1902,06	1486,64	490,01
Mean length (m)	755,42	328,36	253,11	745,87	726,11	301,32	227,72	94,45	588,45	320,63	239,27	97,66
Median length (m)	547,21	242,74	179,90	637,60	562,27	242,65	186,30	79,67	480,25	274,08	211,12	83,08

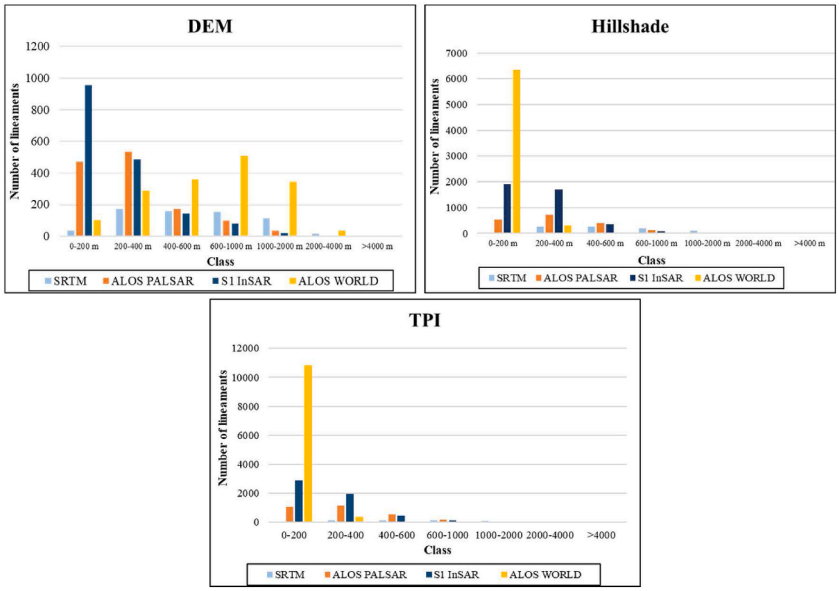

Fig. 17. Histograms of distribution highlighting the lengths of lineaments based on different Digital Elevation Models (DEMs) and methods: Direct DEM extraction (a), TPI (b), and Hillshade (c).

It is worth noting that lineaments of shorter lengths, as indicated in Table 2, are predominantly present in the study area. They represent 30%, 66.16%, and 73.40% of the total number of lineaments extracted using DEMs, Hillshade, and TPI, respectively. This prevalence can be attributed to the presence of ancient rock formations dating back to the Neoproterozoic in the study area, such as metabasalts, metatuffs, serpentines, and biotite-eye gneisses. These rocks have undergone two significant phases of ductile deformation under metamorphic conditions (Soliman and Han, 2019). The nature of these geological formations may explain the increased frequency of shorter lineaments, highlighting the influence of local geological features on the distribution of lineaments in the study area.

4.3. Accuracy assessment

As part of the accuracy assessment, it is imperative to determine the extent to which the extracted lineaments faithfully reflect the geospatial reality. The accuracy assessment relies on a comparison between the lineaments identified by the analysis methods and a ground truth reference, often derived from existing data or previous analyses. This evaluation aims to quantify the precision of lineament detection, highlighting the strengths and weaknesses of each method used.

4.3.1. Lineament density evaluation

Lineament density mapping was created by integrating automatically extracted lineaments from different methods, accompanied by a detailed assessment of their length in each grid cell. This approach aims to reveal nuances in the spatial variation of lineament density within the study area, providing a detailed insight into the geospatial distribution of these topographic features.

Analysis of lineament density results reveals significant trends in the spatial distribution of topographic features within the study area. The category of very low density, which predominates in the larger extent of the area, suggests a prevalence of regions with low lineament density. However, it is essential to pay particular attention to the geological or geomorphological interpretation of these areas, as low density does not necessarily imply an absence of relevant linear features.

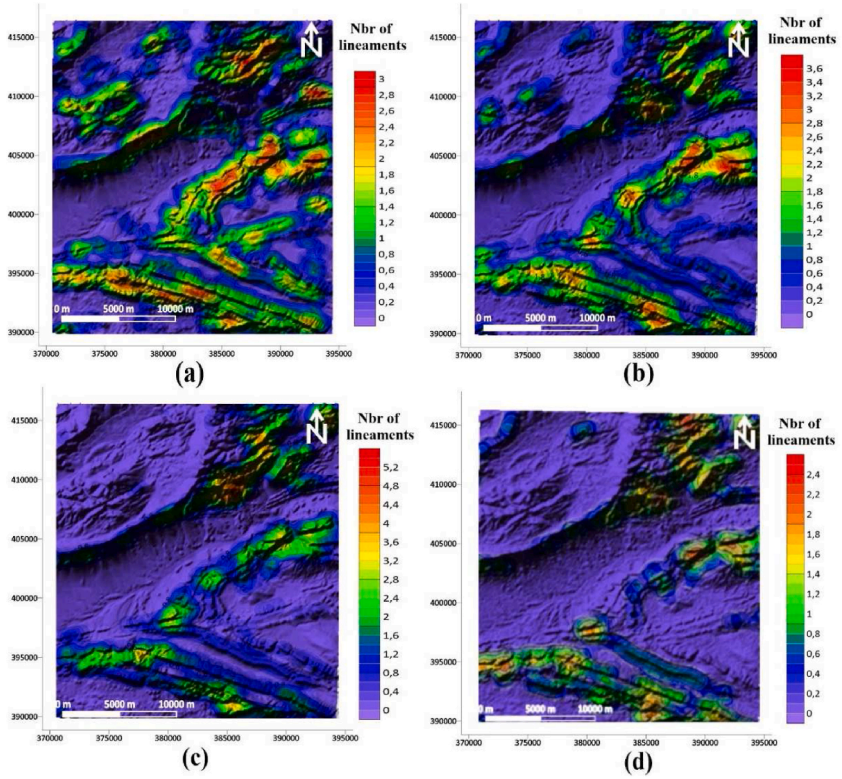

Fig. 18. Lineament density maps automatically extracted from various DEMs: SRTM (a), ALOS PALSAR (b), S1 InSAR (c), and ALOS WORLD (d).

Regarding the extraction method from DEMs (Fig. 18), the SRTM DEM (Fig. 18a) and ALOS PALSAR (Fig. 18b) exhibit more pronounced lineament density anomalies than others, consistent with their increased efficiency in extracting a larger number of lineaments. High frequencies of lineaments are observed in the southern, eastern, and northeastern parts of the study area.

The hillshade method has also demonstrated its effectiveness in lineament extraction, as evidenced by the high frequencies observed in the lineaments extracted from the SRTM DEM (Fig. 19a). These lineaments, already characterized by their significant size, exhibited abnormally high densities in the south and northeast of the study area (Fig. 19).

The TPI method (Fig. 20) stands out for its efficiency in extracting small-sized lineaments, with a frequency mainly concentrated in the North, East, and South regions of the area.

4.3.2. Evaluation of lineament orientation

In this dedicated section for the evaluation of lineament orientation, we explore how these topographic features align and distribute themselves in the study area. The assessment of orientation provides crucial insights into the geological and tectonic structuring, allowing for a better understanding of the processes that have shaped the landscape. By analyzing the predominant direction of lineaments extracted from various DEMs, our objective is to reveal significant directional trends and shed light on the geospatial implications of these orientations.

Regarding the extraction method from the DEMs (Fig. 21), we observe a general East-West orientation. For the Hillshade method (Fig. 22), the lineaments show preferred orientations of NE-SW and N-S. Concerning the TPI method (Fig. 23), the predominant directions are NE-SW and E-W.

The main trend of the rose diagram produced by the Hillshade (Fig. 22) method differs from those of the other two methods due to the specific direction parameters used in this method. For the Hillshade method, a direction of N90 was chosen to extract lineaments in this specific direction which are already documented in the bibliography. This approach highlights the north-south oriented lineaments, which explains the difference observed compared to the other methods that did not use this particular direction for lineament extraction. This variation is intentional and aims to explore the impact of illumination direction on lineament detection. By choosing different illumination orientations, it is possible to highlight lineaments that might not be visible with other orientations. This demonstrates the importance of illumination direction in lineament analysis and explains the observed differences in the trends of the Rose diagrams produced by the Hillshade method compared to the other methods.

These observations lead us to emphasize that even the most extensive lineaments in the study area exhibit similar orientations. However, it is relevant to note that the maps of linements lengths, based on lineaments extracted from different DEMs, reveal distinct directional variations (Fig. 24). In the southern part, lineaments are particularly long, reaching remarkable lengths of up to 11 km according to the SRTM DEM (Fig. 24a), with a predominant orientation of E-W and NE-SW. The Hillshade method also shows a notable concentration of longer lineaments, especially to the east and south of the study area (Fig. 25). The N-S orientation of the extracted

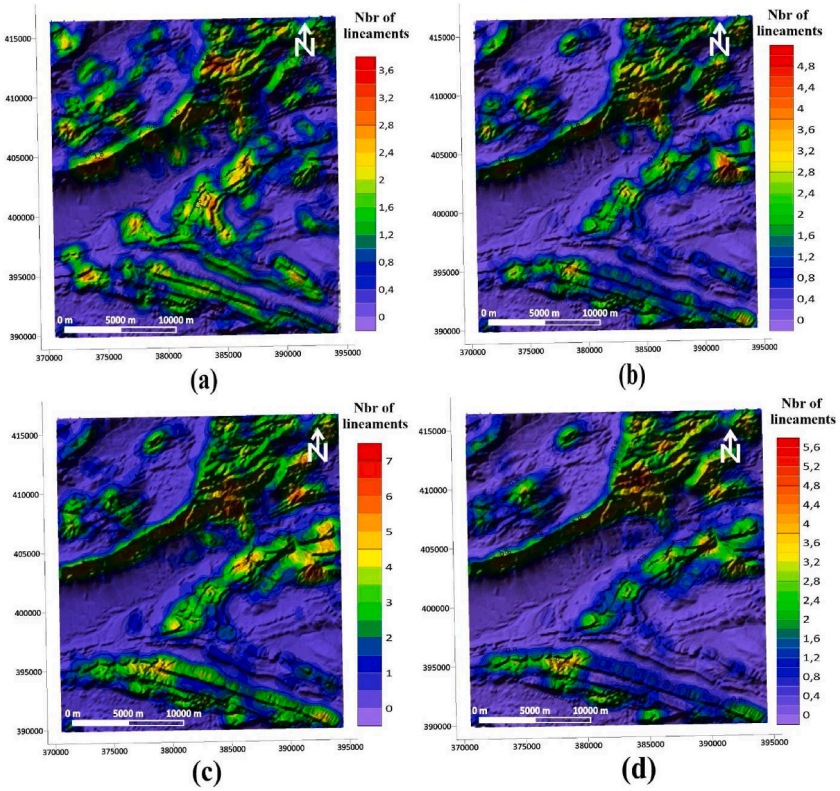

Fig. 19. Lineament density maps automatically extracted from various DEMs using the hillshade method: SRTM (a), ALOS PALSAR (b), S1 InSAR (c), and ALOS WORLD (d).

lineaments corresponds to the specific direction of the Hillshade used (N90). As for the TPI method, it reveals longer lineaments in the southern, eastern, and northern regions (Fig. 26), characterized by lengths exceeding 5 km according to the SRTM data (Fig. 26a). The convergence of the four DEMs toward an E-W direction emphasizes consistency in the directional distribution of lineaments.

5. Discussion

An automated method for extracting lineaments has been successfully applied in the mountainous region of Ait Semgane, enabling the identification of all linear features without distinction between those of natural and anthropogenic origin. The automated lineament extraction methodology, based on various DEMs, TPI, and Hillshade, underwent a comprehensive comparative analysis to determine the optimal method and DEM best suited for lineament extraction in the study area. This evaluation was particularly crucial given the diversity of topographic features and fault orientations in the region, characterized by N-S, NE-SW, and E-W faults according to the literature.

The results highlight a diversity of performance among the analysis methods, underscoring the importance of a strategic approach in selecting the method and datasets based on the specific objectives of the geospatial study. Regarding the number of detected lineaments, the TPI and Hillshade methods proved particularly sensitive, providing a detailed perspective on the linear features of the terrain. Additionally, the ALOS PALSAR and S1 InSAR datasets demonstrated a superior ability to identify subtle linear features, proving especially useful for detailed geomorphological analyses. Simultaneously, the use of SRTM with all three methods facilitated the detection of large-scale lineaments.

The analysis of lineament lengths revealed distinct trends depending on the method and datasets. The TPI and Hillshade methods exhibited a prevalence of shorter lineaments on average, indicating sensitivity to small to medium-scale features. In contrast, the ALOS WORLD DEM distinguished itself by its ability to detect smaller-sized lineaments. Beyond 2000 m, the categories of lineament lengths showed more modest results.

The maps depicting lineament lengths bring attention to specific orientations, revealing a noteworthy concentration of lineaments in the southern region, extending up to considerable lengths of 11 km using the SRTM for the direct extraction method from various DEMs. The Hillshade method identifies a significant concentration of longer lineaments in the eastern and southern sectors, whereas the TPI method accentuates the presence of lineaments.

The results of the assessment of lineament density reveal significant trends in the spatial distribution of these topographic features in the study area. Extraction from DEMs shows a high density in the southern and eastern parts, indicating a general E-W orientation. The TPI method stands out for its effectiveness, presenting a moderate to high density in NE-SW and E-W directions, mainly in the

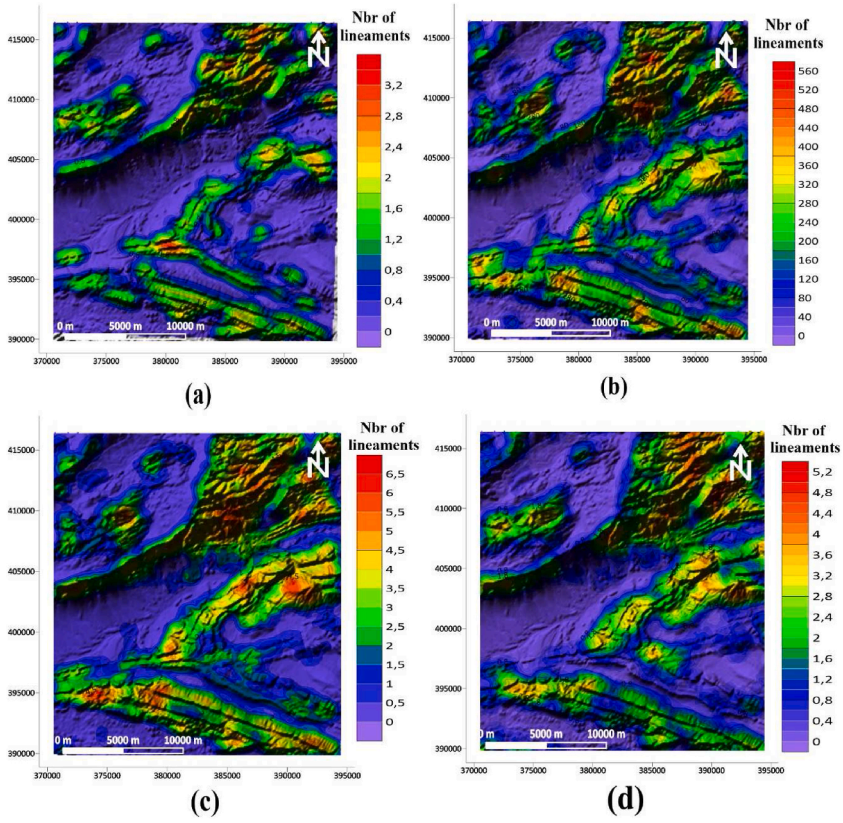

Fig. 20. Density maps of lineaments automatically extracted from various DEMs using the TPI method: SRTM (a), ALOS PALSAR (b), S1 InSAR (c), and ALOS WORLD (d).

north, east, and south. Similarly, the Hillshade method demonstrates its relevance, with high densities in the lineaments of the SRTM DEM and S1 InSAR DEM, showing preferential NE-SW and N-S orientations.

The in-depth analysis of the orientation of lineaments extracted within the study area reveals a remarkable coherence with established geological knowledge found in the literature. The identified orientations, especially the prevalence of lineaments in an E-W, N-S, and NE-SW direction, significantly align with documented tectonic patterns in specialized literature (Riser, 1988) (Missenard) (Abderrahmane et al., 2003). The major deformation event in the region, identified during event PA2, is characterized by vertically inclined faults towards the south, with lineations indicating a predominant overlap under a principal stress direction of NE-SW.

It is noteworthy that the ancient Neoproterozoic rocks in the study area, found in the Bou Azzer-El Graara anticlinorium in the south and in certain northern regions, consist of meta-basalts, metavolcanic tuffs, serpentines, and augen biotite gneisses. These formations have recorded two significant phases of ductile deformations (PA1 and PA2) under conditions of greenschist metamorphism (Hefferan et al., 2000). The oldest schistosity in these rocks is characterized by an E-W and ESE orientation, largely defined by minerals such as chlorite, biotite, talc, and serpentine (Hefferan et al., 2000).

The PA2 phase induced upright to isoclinal folds in the Tiddiline series, oriented NW-SE, with fold axes gently plunging towards the NW (Benssaou and Hamoumi, 1999). This deformation is associated with a left lateral transgression along major faults bordering the ophiolitic sequences at the level of Lower Neoproterozoic formations (Soulaimani et al., 1997). The Hercynian deformation in the area generated widespread fracture cleavage and upright folding in Paleozoic rocks (H1) (Soulaimani et al., 1997). This deformation period is characterized by an E-W direction with a slight dip, upright folds, and block tectonics in the cover (Benssaou and Hamoumi, 1999). The Hillshade method, using a direction of 90°, has demonstrated its effectiveness in extracting north-south-oriented lineaments. These lineaments correspond to the Pan-African events PA3, resulting from faults present in Neoproterozoic-dated facies. These geological formations mainly comprise pelites, sandstones, and conglomerates.

Each method and type of satellite image used in this study presents distinct advantages and disadvantages, highlighting the importance of choosing the appropriate approach based on the specific objectives of the geospatial analysis.

The direct extraction method simplifies the process by directly using DEMs to identify large-scale lineaments. Its primary advantage lies in its efficiency in detecting large linear structures, making it a suitable choice for an overview of the terrain. However, it may lack fine detail and fail to identify smaller lineaments, limiting its ability to provide a detailed analysis of topographic features.

The TPI method stands out for its sensitivity to small to medium-scale features, offering detailed perspectives on terrain characteristics. It is particularly useful for detecting a large number of short lineaments, providing a detailed view of minor topographic varia-

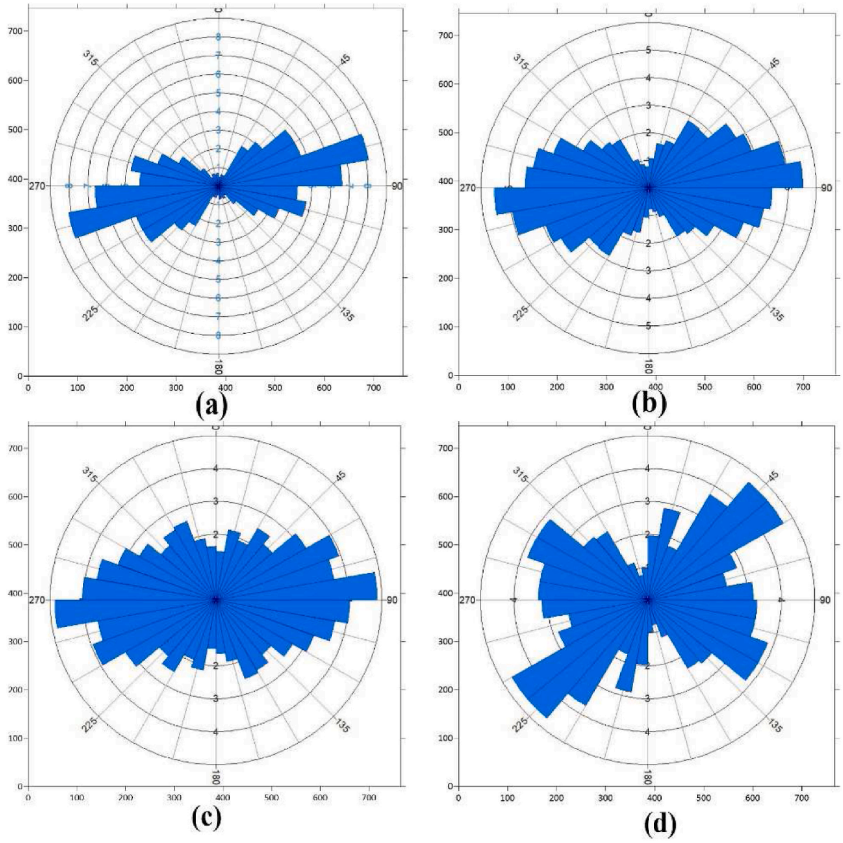

Fig. .21. Rose diagramss showing the main trends obtained for the automatic extraction of lineaments directly from different DEMs: SRTM (a), ALOS PALSAR (b), S1 InSAR (c), and ALOS WORLD (d).

tions. However, this increased sensitivity can also be a disadvantage, as it may lead to an overabundance of short lineaments, complicating the overall interpretation.

On the other hand, the Hillshade method is effective in identifying lineaments oriented in specific directions, such as north-south lineaments. By using an illumination direction of 90°, it highlights lineaments in this orientation, which aligns with documented geological events. However, its dependence on the chosen illumination direction can introduce bias in the detection of lineaments, limiting its ability to identify features in other orientations.

Regarding satellite images, each type also presents specific advantages and limitations. SRTM is particularly well-suited for detecting large-scale lineaments, offering an overview of the terrain. It is most effective for identifying large structures, making it an ideal choice for large-scale analysis. However, it may overlook smaller features and lack the sensitivity needed to detect fine details, compared to higher-resolution data such as that provided by ALOS PALSAR and S1 InSAR.

ALOS PALSAR is superior for identifying subtle linear features, making it particularly useful for detailed geomorphological analyses. It is capable of detecting minor lineaments with high precision. However, it may be limited in detecting large-scale lineaments, where SRTM might be more effective.

Like ALOS PALSAR, S1 InSAR excels in detecting fine details and small features, enhancing the detection of minor lineaments. However, this increased precision for small lineaments means it may be less effective in identifying large linear structures, limiting its use for large-scale analyses.

ALOS WORLD DEM is effective for detecting small-sized lineaments, complementing other datasets for a comprehensive analysis. However, similar to ALOS PALSAR and S1 InSAR, it may be limited in detecting larger lineaments compared to SRTM.

The analysis of these different extraction methods and satellite data, along with the mapping of faults presented on the geological map of Ait Semgane, was conducted by comparing them to various automatically extracted lineaments. This approach has clearly highlighted the combined success of the SRTM DEM model and the TPI method in extracting the most significant lineaments, as detailed in Fig. 27a. Furthermore, this methodology has yielded significant results regarding the spatial distribution of faults and their predominant orientations, as explicitly shown in Fig. 27b and c.

It is particularly noteworthy that the most extensive faults are concentrated in the northwest and south sectors of the area, aligning along the E-O and ENE-OSO directions. This observation consistently aligns with bibliographic references, thereby reinforcing the validity and reliability of the undertaken cartographic analysis. It is also worth emphasizing that this automated methodology enabled the extraction of lineaments in structurally unmapped areas, especially in the SE and NW parts of the study area.

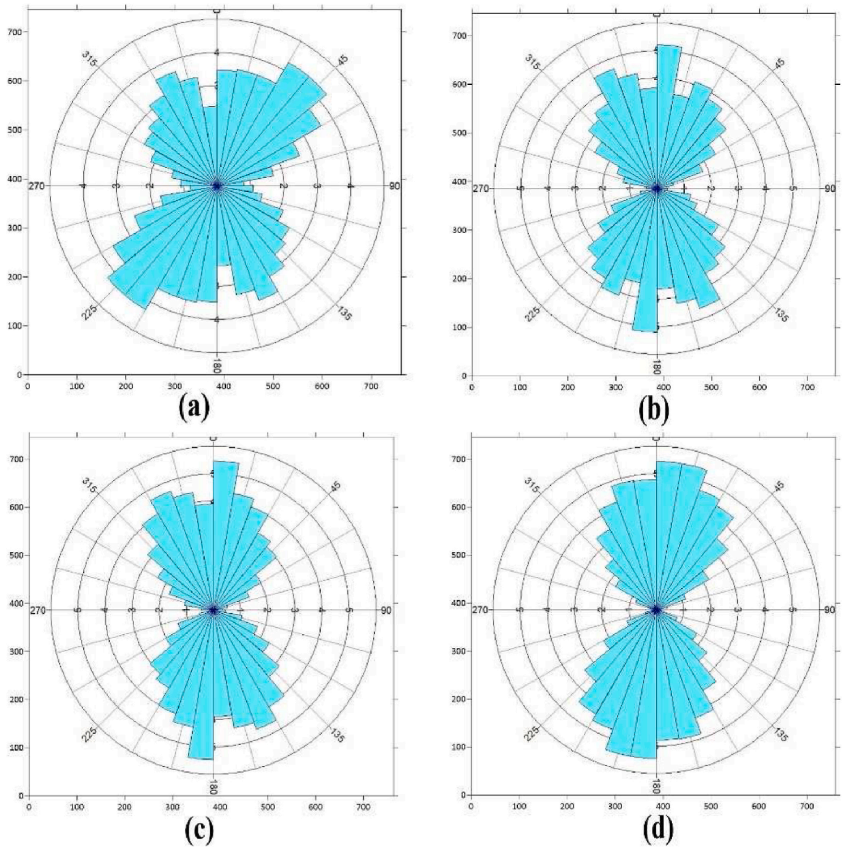

Fig. 22. Rose diagrams showing the main trends obtained for the automatic extraction of lineaments using the Hillshade method: SRTM (a), ALOS PALSAR (b), S1 InSAR (c) et ALOS WORLD (d).

The accuracy assessment has shed light on the need to determine the extent to which the extracted lineaments faithfully reflect the geospatial reality. This in-depth analysis has provided insights into the spatial distribution of topographic features. The results have been supported by comparisons with existing geological data, thereby reinforcing the validity of the conclusions drawn. Crucially, these conclusions have been validated in the field, further enhancing the reliability of the obtained results (Fig. 27 d, e, f, g, et h).

6. Conclusion

The automation of linear feature extraction in a given area is closely tied to the resolution of the data used and the employed methodology. Technologies such as SRTM, ALOS PALSAR, S1 InSAR, and ALOS WORLD, coupled with TPI, Hillshade, and direct extraction methods from DEMs, prove to be crucial tools for mapping morphostructural lineaments, especially in challenging and less accessible areas. These approaches help overcome limitations inherent in software parameters and algorithmic constraints.

Analyzing lineaments, with a focus on areas of high and very high density, combined with other morphostructural indicators, provides compelling evidence of structural deformations within the study area. The obtained results demonstrate orientations and magnitudes consistent with structures previously mapped in existing geological data, thereby enriching the lineament database for the Ait Semgane region.

The correlation between the size of lineaments and the type of morphology and rock formation in the study area is particularly significant. Larger lineaments, often associated with major faults and tectonic structures, are primarily detected using the SRTM dataset, which excels in capturing large-scale topographic features. These large lineaments correlate well with prominent geological structures and major fault lines documented in the region. For instance, the large lineaments detected align with the major Eburnean, Pan-African, and Hercynian orogenies, which have significantly shaped the Anti-Atlas region.

Conversely, smaller lineaments, identified effectively through the ALOS WORLD and TPI methods, are indicative of finer structural details and minor faults. These smaller features are often found in areas with complex morphologies, such as highly fractured rock formations and regions with significant erosion. The high resolution of these datasets enables the detection of smaller structural features that might be overlooked by lower-resolution methods.

The diversity in lineament sizes, coupled with the varying sensitivities of the employed methods, provides a comprehensive understanding of the geological framework. The SRTM data's ability to reveal large-scale structures complements the detailed, fine-scale in-

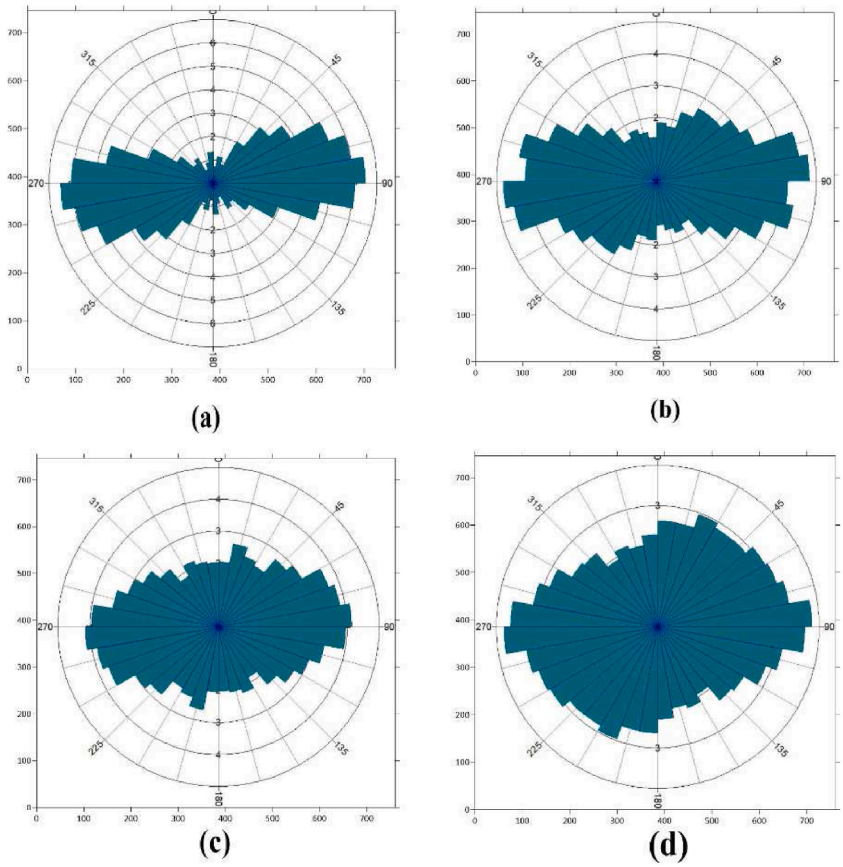

Fig. 23. Rose diagrams showing the main trends obtained for the automatic extraction of lineaments using the TPI method: SRTM (a), ALOS PALSAR (b), S1 InSAR (c) et ALOS WORLD (d).

formation obtained from the ALOS WORLD and TPI methods, offering a robust approach to mapping and analyzing the morphostructural characteristics of the study area.

This innovative methodology proves to be an effective means of extracting and analyzing geological lineaments in extensive and hard-to-reach regions, even in areas with generally limited outcrops. While specific targeted field observations (as shown in Fig. 27) may demonstrate localized areas with more frequent outcrops, the overall region may still pose significant challenges for direct observation. Its use optimizes time and reduces costs associated with collecting structural information, particularly relevant in the early stages of geological, civil, and mining exploration.

The main conclusions of this study highlight several key points:

- TPI stands out for its ability to facilitate more precise and reliable extraction of linear features.
- ALOS WORLD, combined with the TPI method, allows for the efficient extraction of short-length lineaments.
- Resolution plays a crucial role, with SRTM being particularly relevant for extracting larger-sized lineaments.
- The Hillshade method is limited by the chosen initial direction, underscoring the importance of this parameter in the process.

The entirety of these results clearly attests to the synergistic success achieved through the combined application of the SRTM DEM model and the TPI method in extracting the most significant lineaments, thereby reinforcing the validity and effectiveness of the adopted approach.

Ethical statement

Hereby, I/Ali shebl/consciously assure that for the manuscript/Optimization of Lineament Extraction: Analysis and Comparison of Digital Elevation Models/the following is fulfilled:

1) This material is the authors' own original work, which has not been previously published elsewhere.
2) The paper is not currently being considered for publication elsewhere.
3) The paper reflects the authors' own research and analysis in a truthful and complete manner.
4) The paper properly credits the meaningful contributions of co-authors and co-researchers.
5) The results are appropriately placed in the context of prior and existing research.

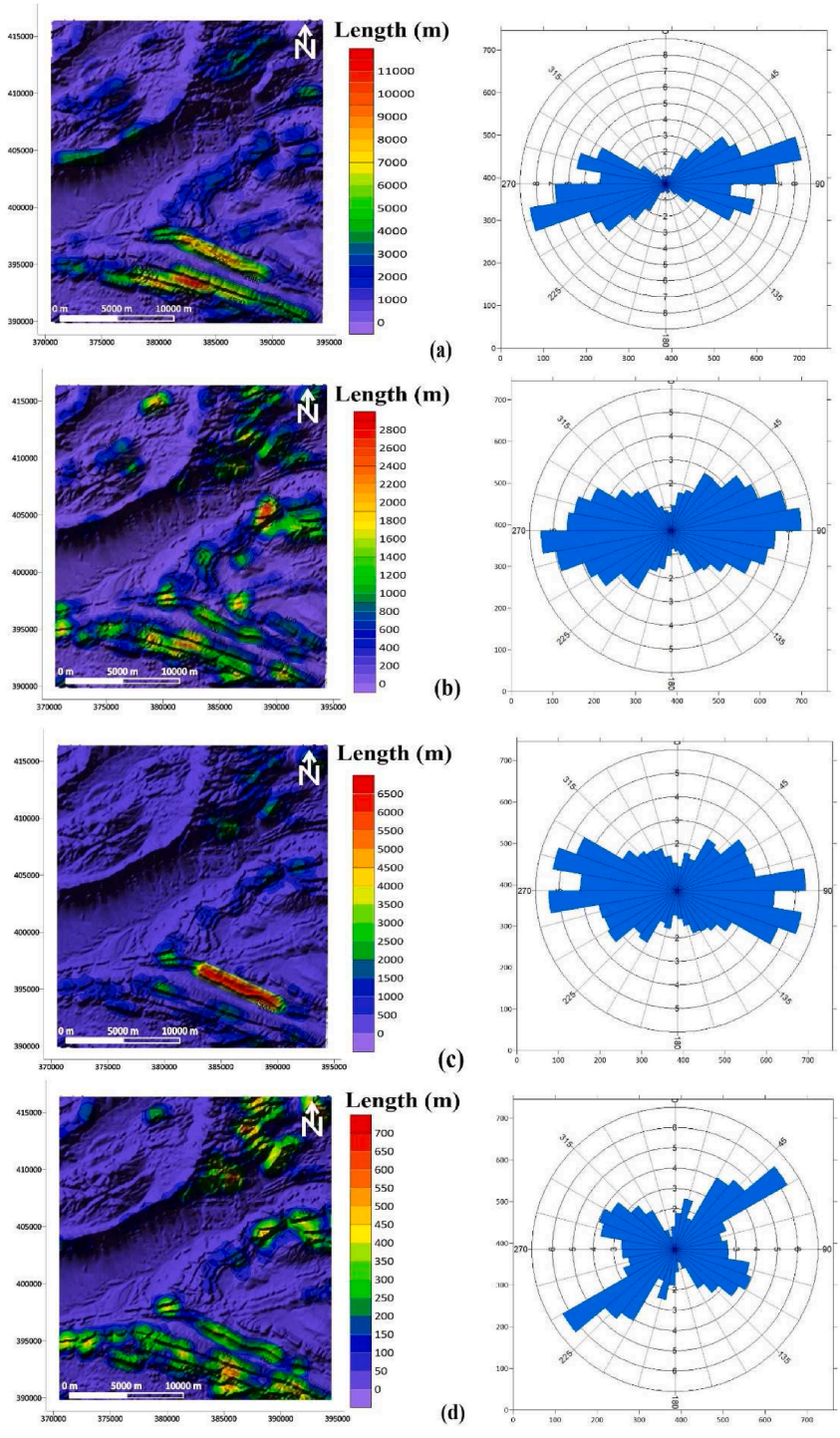

Fig. 24. Length maps of automatically extracted linear features from various DEMs, accompanied by their Rose diagrams: SRTM (a), ALOS PALSAR (b), S1 InSAR (c) et ALOS WORLD (d).

6) All sources used are properly disclosed (correct citation). Literally copying of text must be indicated as such by using quotation marks and giving proper reference.
7) All authors have been personally and actively involved in substantial work leading to the paper, and will take public responsibility for its content.

I agree with the above statements and declare that this submission follows the policies of Solid State Ionics as outlined in the Guide for Authors and in the Ethical Statement.

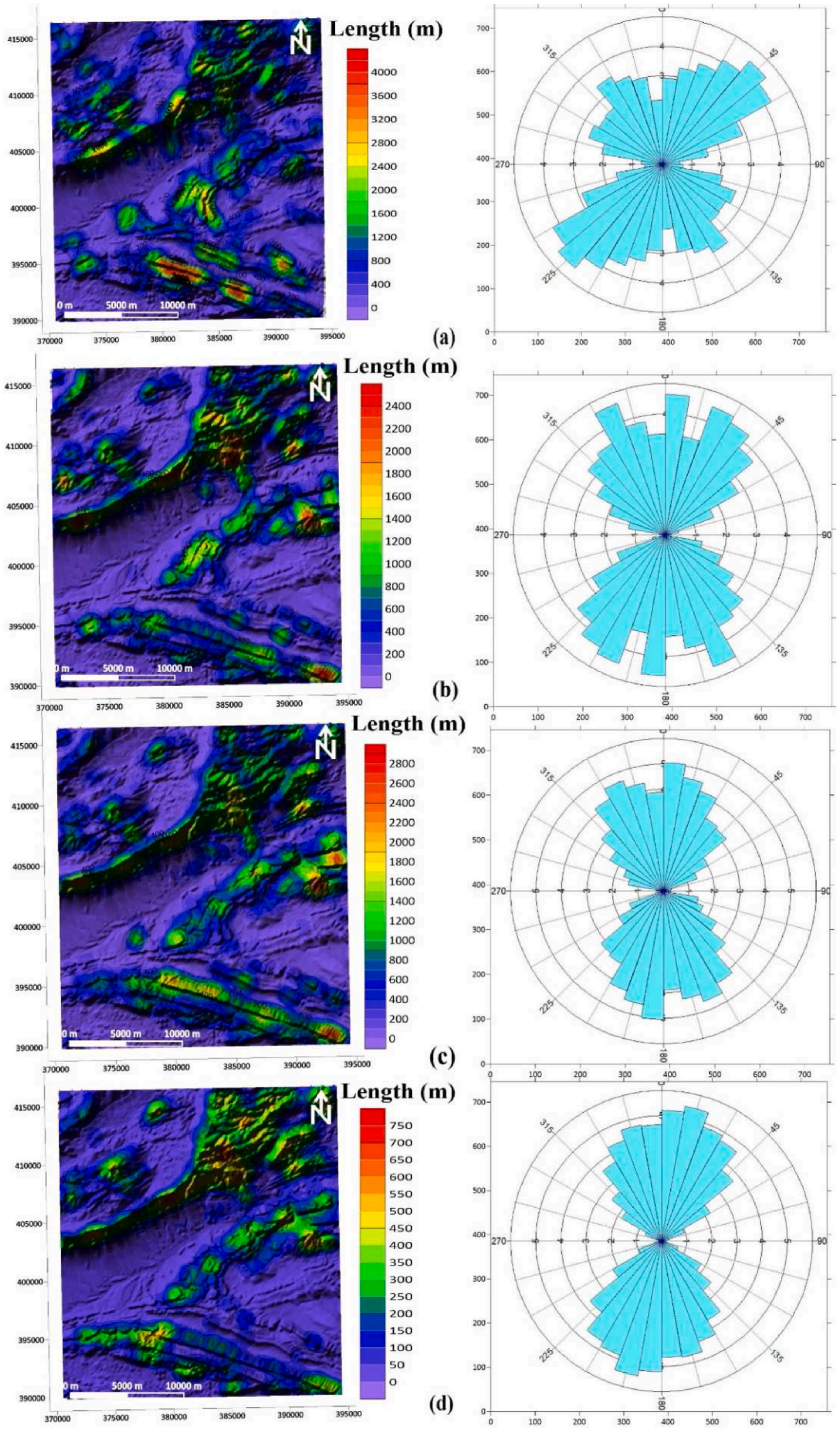

Fig. 25. Length maps of automatically extracted linear features using the Hillshade method, accompanied by their Rose diagrams: SRTM (a), ALOS PALSAR (b), S1 In-SAR (c) et ALOS WORLD (d).

CRediT authorship contribution statement

Mohamed Ali EL-Omairi: Writing – original draft, Software, Methodology, Formal analysis, Data curation, Conceptualization. **Abdelkader El Garouani:** Writing – review & editing, Software, Resources, Project administration, Investigation. **Ali Shebl:** Writing – review & editing, Validation, Funding acquisition.

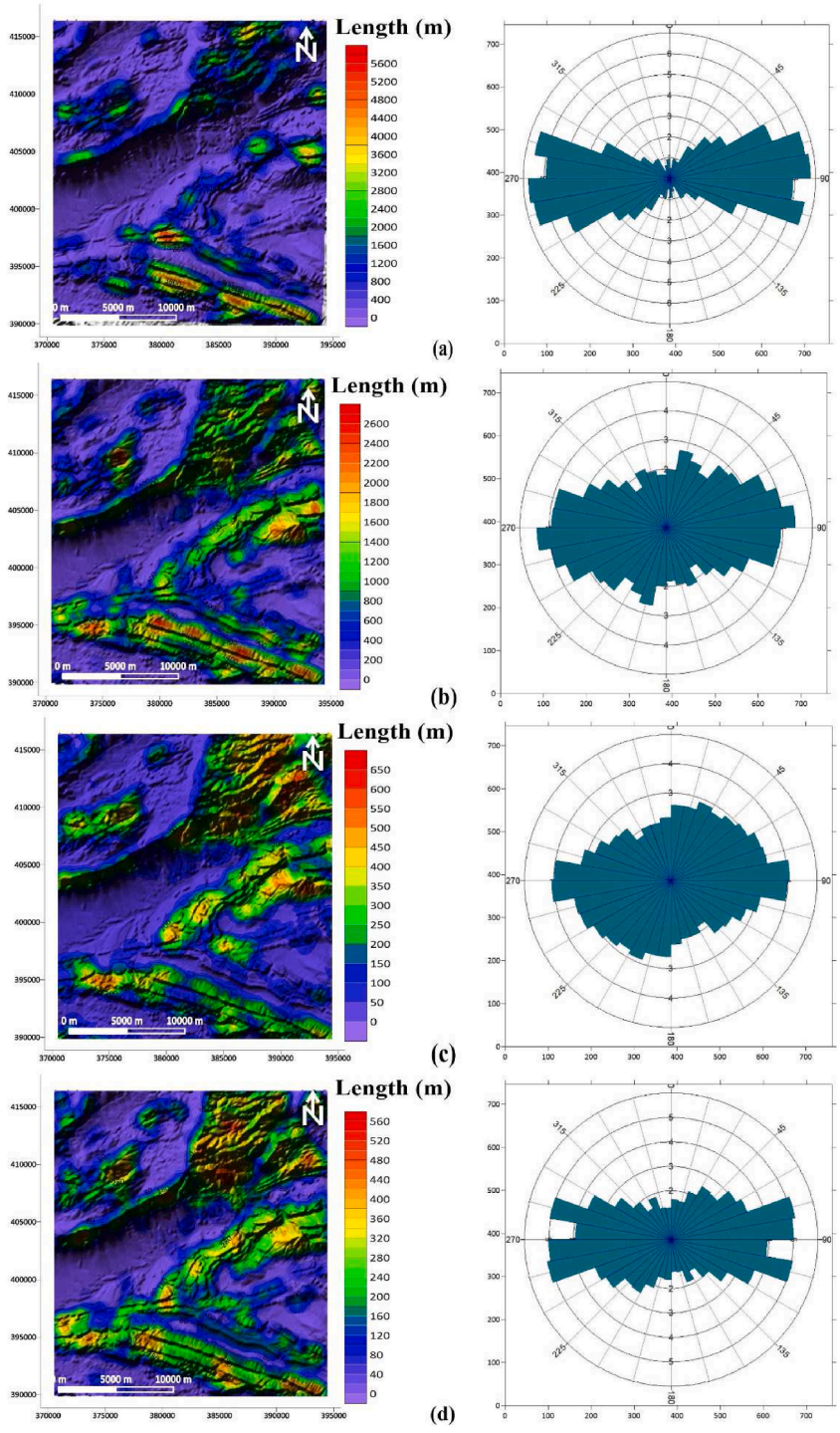

Fig. 26. Length maps of automatically extracted linear features using the TPI method, accompanied by their Rose diagrams: SRTM (a), ALOS WORLD (b), ALOS PALSAR (c) et S1 InSAR (d).

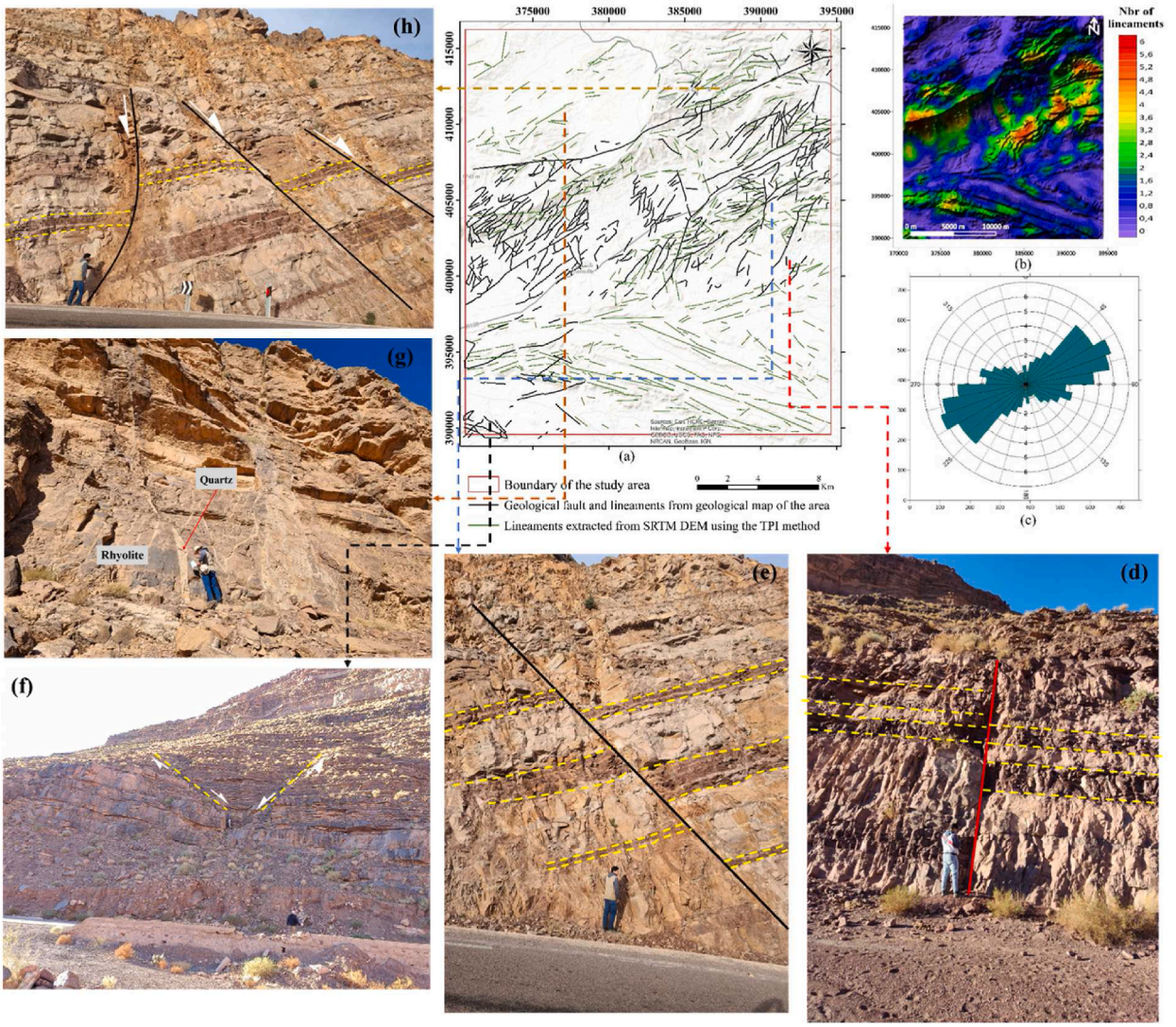

Fig. 27. Fault and geological lineament mapping in the study area (a), density map using TPI method and SRTM DEM (b) accompanied by their rose diagram (c). Ground-truth observations of linear features, including vertical normal fault (d) N48° oriented normal fault (e), representation of a graben associated with two normal faults (f), fractured rhyolites with quartz-filled fractures (g) Central horst with normal faults oriented N124° with a dip of 50° to the northwest in argillite and sandstone strata (h).

Declaration of competing interest

The authors declare that they have no known competing financial interests or personal relationships that could have appeared to influence the work reported in this paper.

Data availability

Data will be made available on request.

References

Abdelkareem, M., Bamousa, A.O., Hamimi, Z., Kamal El-Din, G.M., 2020. Multispectral and RADAR images integration for geologic, geomorphic, and structural investigation in southwestern Arabian Shield, Al Qunfudhah area, Saudi Arabia. J. Taibah Univ. Sci. 14 (1), 383–401. https://doi.org/10.1080/16583655.2020.1741957.

Abderrahmane, S., Bouabdelli, M., Piqué, A., 2003. L'extension continentale au Néo-Protérozoïque supérieur-Cambrien inférieur dans l'Anti-Atlas (Maroc) The Upper Neoproterozoic-Lower Cambrian continental extension in the Anti-Atlas (Morocco). Bull. Soc. Geol. Fr. 174, 83–92.

Abdullah, A., Akhir, J.M., Abdullah, I., 2010. The Extraction of Lineaments Using Slope Image Derived from Digital Elevation Model: Case.

Admou, H., 2011. MASSIF DU SIROUA. pp. 83–104.

M. Agoussine, M. E. M. Saidi, and B. Igmoullan, "Reconnaissance des ressources en eau du bassin d'Ouarzazate (Sud-Est marocain)".

Ahmadi, H., Pekkan, E., 2021. Fault-based geological lineaments extraction using remote sensing and GIS—a review. Geosciences 11 (5), 183. https://doi.org/10.3390/geosciences11050183.

Altinoğlu, F.F., Sari, M., Aydin, A., 2015. Detection of lineaments in denizli basin of western anatolia region using bouguer gravity data. Pure Appl. Geophys. 172 (2), 415–425. https://doi.org/10.1007/s00024-014-0911-y.
Anbalagan, R., 1992. Landslide hazard evaluation and zonation mapping in mountainous terrain. Eng. Geol. 32 (4), 269–277. https://doi.org/10.1016/0013-7952(92)90053-2.
Anbalagan, R., Singh, B., 1996. Landslide hazard and risk assessment mapping of mountainous terrains — a case study from Kumaun Himalaya, India. Eng. Geol. 43 (4), 237–246. https://doi.org/10.1016/S0013-7952(96)00033-6.
Bajja, A., 1987. Nouvelles données pétrographiques et géochimiques sur les formations volcaniques précambriennes du Djebel Saghro (anti-atlas marocain), basaltes en coussins du P II et volcanites de la série de Ouarzazate (P III). [Online]. Available: https://www.semanticscholar.org/paper/Nouvelles-donn%C3%A9es-p%C3%A9trographiques-et-g%C3%A9ochimiques-P-Bajja/b448e7908ccc7b0889407ee74d769553b4d6cb58. (Accessed 21 November 2023).
Batchelor, R.A., Bowden, P., 1985. Petrogenetic interpretation of granitoid rock series using multicationic parameters. Chem. Geol. 48 (1–4), 43–55. https://doi.org/10.1016/0009-2541(85)90034-8.
Benssaou, M., Hamoumi, N., 1999. L'Anti-Atlas occidental du Maroc : remplissage sédimentaire d'un bassin de type rift intracontinental au Cambrien inférieur. Geol. Mediterr. 26 (3), 259–279. https://doi.org/10.3406/geolm.1999.1661.
Bourjila, A., et al., 2021. Groundwater potential zones mapping by applying GIS, remote sensing and multi-criteria decision analysis in the Ghiss basin, northern Morocco. Groundw. Sustain. Dev. 15, 100693. https://doi.org/10.1016/j.gsd.2021.100693.
Bufalini, M., Materazzi, M., De Amicis, M., Pambianchi, G., 2021. From traditional to modern 'full coverage' geomorphological mapping: a study case in the Chienti river basin (Marche region, central Italy). J. Maps 17 (3), 17–28. https://doi.org/10.1080/17445647.2021.1904020.
Cardoso-Fernandes, J., Teodoro, A.C., Lima, A., Menuge, J., Brönner, M., Steiner, R., 2022. Sentinel-1 and ALOS data for lineament extraction: a comparative study. In: Earth Resources and Environmental Remote Sensing/GIS Applications XIII. pp. 221–238. https://doi.org/10.1117/12.2636117SPIE.
De Reu, J., et al., 2013. Application of the topographic position index to heterogeneous landscapes. Geomorphology 186, 39–49. https://doi.org/10.1016/j.geomorph.2012.12.015.
D'Lemos, R.S., Inglis, J.D., Samson, S.D., 2006. A newly discovered orogenic event in Morocco: neoproterozic ages for supposed Eburnean basement of the Bou Azzer inlier, Anti-Atlas Mountains. Precambrian Res. 147 (1), 65–78. https://doi.org/10.1016/j.precamres.2006.02.003.
El-Naqa, A., Hammouri, N., Ibrahim, K., Al-Taj, M., 2010. Integrated approach for groundwater exploration in wadi araba using remote sensing and GIS. Jordan J. Civ. Eng. 3.
Elmahdy, S.I., Mohamed, M.M., Ali, T.A., 2021. Automated detection of lineaments express geological linear features of a tropical region using topographic fabric grain algorithm and the SRTM DEM. Geocarto Int. 36 (1), 76–95. https://doi.org/10.1080/10106049.2019.1594393.
Emran, A., Chorowicz, J., 1992. La tectonique polyphasée dans la boutonnière précambrienne de Bou Azzer (Anti-Atlas central, Maroc) : apports de l'imagerie spatiale Landsat-MSS et de l'analyse structurale de terrain/The Panafrican tectonic events in the eroded anticline of Bou Azzer (Central Anti-Atlas, Morocco), from Landsat-MSS imagery and field structural analysis. Sci. Géologiques Bull. Mém. 45 (2), 121–134. https://doi.org/10.3406/sgeol.1992.1888.
Es-sabbar, B., Essalhi, M., Essalhi, A., Si Mhamdi, H., 2020. Lithological and structural lineament mapping from landsat 8 OLI images in ras kammouna arid area (eastern anti-atlas, Morocco). Econ. Environ. Geol. 4, 425–440. https://doi.org/10.9719/EEG.2020.53.4.425.
Farmakis-Serebryakova, M., Hurni, L., 2020. Comparison of relief shading techniques applied to landforms. ISPRS Int. J. Geo-Inf. 9 (4), 253. https://doi.org/10.3390/ijgi9040253.
Choubert, G.A., 1986. Histoire géologique du précambrien de l'Anti-Atlas. In: du service géologique du Maroc. [Rabat], 1963.
Ghosh, S., Sivasankar, T., Anand, G., 2021. Performance evaluation of multi-parametric synthetic aperture radar data for geological lineament extraction. Int. J. Rem. Sens. 42 (7), 2574–2593. https://doi.org/10.1080/01431161.2020.1856963.
Görler, K., et al., 1988. The uplift of the central High Atlas as deduced from neogene continental sediments of the Ouarzazate province, Morocco. In: Jacobshagen, V.H. (Ed.), Lecture Notes in Earth Sciences, 15. Springer-Verlag, Berlin/Heidelberg, pp. 359–404. https://doi.org/10.1007/BFb0011601.
Hashim, M., Ahmad, S., Johari, M.A.M., Pour, A.B., 2013. Automatic lineament extraction in a heavily vegetated region using Landsat Enhanced Thematic Mapper (ETM+) imagery. Adv. Space Res. 51 (5), 874–890. https://doi.org/10.1016/j.asr.2012.10.004.
Hefferan, K.P., Admou, H., Karson, J.A., Saquaque, A., 2000. Anti-atlas (Morocco) role in neoproterozoic western gondwana reconstruction. Precambrian Res. 103 (1), 89–96. https://doi.org/10.1016/S0301-9268(00)00078-4.
HOBBS, W.H., 1904. Lineaments of the atlantic border region. GSA Bull. 15 (1), 483–506. https://doi.org/10.1130/GSAB-15-483.
Horn, B.K.P., 1981. Hill shading and the reflectance map. Proc. IEEE 69 (1), 14–47. https://doi.org/10.1109/PROC.1981.11918.
Javhar, A., et al., 2019. Comparison of multi-resolution optical landsat-8, sentinel-2 and radar sentinel-1 data for automatic lineament extraction: a case study of alichur area, SE pamir. Rem. Sens. 11 (7), 778. https://doi.org/10.3390/rs11070778.
Jordan, G., Meijninger, B.M.L., Hinsbergen, D.J.J.V., Meulenkamp, J.E., Dijk, P.M.V., 2005. Extraction of morphotectonic features from DEMs: development and applications for study areas in Hungary and NW Greece. Int. J. Appl. Earth Obs. Geoinformation 7 (3), 163–182. https://doi.org/10.1016/j.jag.2005.03.003.
Knitter, D., Brozio, J.P., Hamer, W., Duttmann, R., Müller, J., Nakoinz, O., 2019. Transformations and site locations from a landscape archaeological perspective: the case of neolithic wagrien, schleswig-holstein, Germany. Land 8 (4), 68. https://doi.org/10.3390/land8040068.
Kokinou, E., Panagiotakis, C., 2020. Automatic pattern recognition of tectonic lineaments in seafloor morphology to contribute in the structural analysis of potentially hydrocarbon-rich areas. Rem. Sens. 12 (10), 1538. https://doi.org/10.3390/rs12101538.
Leblanc, M., 1975. Ophiolites précambriennes et gîtes arsenies de cobalt (Bou Azzer-Maroc). In: Mémoire/Centre géologique et géophysique. Centre géologique et géophysique, Montpellier.
Leblanc, M., Lancelot, J., 2011. Interprétation géodynamique du domaine pan-africain (Précambrien terminal) de l'Anti-Atlas (Maroc) à partir de données géologiques et géochronologiques. Can. J. Earth Sci. 17, 142–155. https://doi.org/10.1139/e80-012.
Lu, P.F., An, Ping, 1999. A metric for spatial data layers in favorability mapping for geological events. IEEE Trans. Geosci. Rem. Sens. 37 (3), 1194–1198. https://doi.org/10.1109/36.763271.
Magaia, L.A., Goto, T., Masoud, A.A., Koike, K., 2018. Identifying groundwater potential in crystalline basement rocks using remote sensing and electromagnetic sounding techniques in central western Mozambique. Nat. Resour. Res. 27 (3), 275–298. https://doi.org/10.1007/s11053-017-9360-5.
Manuel, R., Brito, M.D.G., Chichorro, M., Rosa, C., 2017. Remote sensing for mineral exploration in Central Portugal. Minerals 7 (10). https://doi.org/10.3390/min7100184. Art. no. 10.
A. J. Martial, M. O. Joseph, O. J. Bosco, E. Jean, and M. P. Kemeng, "Utilisation des modèles numériques de terrain (MNT) SRTM pour la cartographie des linéaments structuraux : Application à l'Archéen de Mezesse à l'est de Sangmélima (Sud-Cameroun).".
Y. Missenard, "Le relief des Atlas Marocains: contribution des processus asthénosphériques et du raccourcissement crustal, aspects chronologiques.".
Moustafa, S.S.R., Abdalzaher, M.S., Abdelhafiez, H.E., 2022. Seismo-lineaments in Egypt: analysis and implications for active tectonic structures and earthquake magnitudes. Rem. Sens. 14 (23). https://doi.org/10.3390/rs14236151. 23.
Nahid, A., 2001. Six décenes d'evolution des idées sur les méthodes et concepts en chronostratigraphie du Quaternaire continental marocain: Entre lés dificultés, les incertitudes et le progrés. Cuaternario Geomorfol. Rev. Soc. Esp. Geomorfol. Asoc. Esp. Para El Estud. Cuaternario 15 (1–2), 135–160.
Najafifar, A., Hosseinzadeh, J., Karamshahi, A., 2019. The role of hillshade, aspect, and toposhape in the woodland dieback of arid and semi-arid ecosystems: a case study in zagros woodlands of ilam province, Iran. J. Landsc. Ecol. 12 (2), 79–91. https://doi.org/10.2478/jlecol-2019-0011.
O'Leary, D.W., Friedman, J.D., Pohn, H.A., 1976. Lineament, linear, lineation: some proposed new standards for old terms. Geol. Soc. Am. Bull. 87 (10), 1463. https://doi.org/10.1130/0016-7606(1976)87<1463:LLLSPN>2.0.CO;2.
Rahnama, M., Gloaguen, R., 2014. TecLines: a MATLAB-based toolbox for tectonic lineament analysis from satellite images and DEMs, Part 1: line segment detection and extraction. Rem. Sens. 6 (7). https://doi.org/10.3390/rs6075938. 7.
Ramli, M.F., Yusof, N., Yusoff, M.K., Juahir, H., Shafri, H.Z.M., 2010. Lineament mapping and its application in landslide hazard assessment: a review. Bull. Eng. Geol. Environ. 69 (2), 215–233. https://doi.org/10.1007/s10064-009-0255-5.
Rauf, J., Kayambo, M.R., Nurjana, I., Manyoe, I.N., 2023. Lineament extraction analysis using digital elevation model (DEM) in lahendong geothermal area, north sulawesi. E3S Web Conf. 400, 01009. https://doi.org/10.1051/e3sconf/202340001009.

Riser, J., 1988. Anti-atlas. Encycl. Berbère (5). https://doi.org/10.4000/encyclopedieberbere.2522. 5.
Salui, C.L., 2018. Methodological validation for automated lineament extraction by LINE method in PCI Geomatica and MATLAB based hough transformation. J. Geol. Soc. India 92 (3), 321–328. https://doi.org/10.1007/s12594-018-1015-6.
Shebl, A., Csámer, Á., 2021. Reappraisal of DEMs, Radar and optical datasets in lineaments extraction with emphasis on the spatial context. Remote Sens. Appl. Soc. Environ. 24, 100617. https://doi.org/10.1016/j.rsase.2021.100617.
Shebl, A., Abdellatif, M., Elkhateeb, S.O., Csámer, Á., 2021. Multisource data analysis for gold potentiality mapping of atalla area and its environs, central eastern desert, Egypt. Minerals 11 (6). https://doi.org/10.3390/min11060641. 6.
Sichugova, L., Fazilova, D., 2020. Structural interpretation of lineaments using satellite image processing: a case study in the vicinity of the Charvak reservoir. InterCarto InterGIS 26 (2), 436–442. https://doi.org/10.35595/2414-9179-2020-2-26-436-442.
Sichugova, L., Fazilova, D., 2021. The lineaments as one of the precursors of earthquakes: a case study of Tashkent geodynamical polygon in Uzbekistan. Geod. Geodyn. 12 (6), 399–404. https://doi.org/10.1016/j.geog.2021.08.002.
Šilhavý, J., Minár, J., Mentlík, P., Sládek, J., 2016. A new artefacts resistant method for automatic lineament extraction using Multi-Hillshade Hierarchic Clustering (MHHC). Comput. Geosci. 92, 9–20. https://doi.org/10.1016/j.cageo.2016.03.015.
Sichugova, L., Fazilova, D., 2024. Study of the seismic activity of the Almalyk-Angren industrial zone based on lineament analysis. Int. J. Eng. Geosci. 9 (1), 1–11. https://doi.org/10.26833/ijeg.1192118.
Soliman, A., Han, L., 2019. Effects of vertical accuracy of digital elevation model (DEM) data on automatic lineaments extraction from shaded DEM. Adv. Space Res. 64 (3), 603–622. https://doi.org/10.1016/j.asr.2019.05.009.
Soulaimani, A., Le Corre, Cl, Farazdaq, R., 1997. Déformation hercynienne et relation socle/couverture dans le domaine du Bas-Drâa (Anti-Atlas occidental, Maroc). J. Afr. Earth Sci. 24 (3), 271–284. https://doi.org/10.1016/S0899-5362(97)00043-2.
Takorabt, M., Toubal, A.C., Haddoum, H., Zerrouk, S., 2018. Determining the role of lineaments in underground hydrodynamics using Landsat 7 ETM+ data, case of the Chott El Gharbi Basin (western Algeria). Arabian J. Geosci. 11 (4), 76. https://doi.org/10.1007/s12517-018-3412-y. Feb.
Tang, G., 2014. Progress of DEM and digital terrain analysis in China. Acta Geograph. Sin. 69, 1305–1325. https://doi.org/10.11821/dlxb201409006.
Tende, A., Mustapha, T., Fru, M.I., Gajere, J., Aminu, M., 2022. Hybrid extraction of tectonic lineaments from digital elevation model. Appl. Geomat. 14 (Feb). https://doi.org/10.1007/s12518-022-00422-6.
van der Pluijm, B.A., Van der Pluijm, B.A., Marshak, S., 2004. In: Earth Structure: an Introduction to Structural Geology and Tectonics. International Student, 2. Norton, New York, NY.
Villalta Echeverria, M.D.P., Viña Ortega, A.G., Larreta, E., Romero Crespo, P., Mulas, M., 2022. Lineament extraction from digital terrain derivate model: a case study in the girón–santa isabel basin, south Ecuador. Rem. Sens. 14 (21), 5400. https://doi.org/10.3390/rs14215400.
Walsh, G.J., et al., 2012. Neoproterozoic tectonic evolution of the jebel Saghro and Bou azzer—el Graara inliers, eastern and central anti-atlas, Morocco. Precambrian Res. 216 (219), 23–62. https://doi.org/10.1016/j.precamres.2012.06.010.
Wu, T.-D., Lee, M.T., 2007. Geological lineament and shoreline detection in SAR images. In: 2007 IEEE International Geoscience and Remote Sensing Symposium. pp. 520–523. https://doi.org/10.1109/IGARSS.2007.4422845.
Wu, S., Li, J., Huang, G.H., 2008. A study on DEM-derived primary topographic attributes for hydrologic applications: sensitivity to elevation data resolution. Appl. Geogr. 28 (3), 210–223. https://doi.org/10.1016/j.apgeog.2008.02.006.
Yazidi, A., et al., 2008. Carte géologique au 1/50 000, Feuille Ait Semgane,“ *Notes Mém. Serv. Géologique Maroc*, 472.
Yun, Sang-Ho, Moon, W.M., 2001. Lineament extraction from DEM using drainage network. In: IGARSS 2001. Scanning the Present and Resolving the Future. Proceedings. IEEE 2001 International Geoscience and Remote Sensing Symposium (Cat. No.01CH37217). IEEE, Sydney, NSW, Australia, pp. 2337–2339. https://doi.org/10.1109/IGARSS.2001.977994.
Zhou, Q., 2017. Digital elevation model and digital surface model. In: International Encyclopedia of Geography. John Wiley & Sons, Ltd, pp. 1–17. https://doi.org/10.1002/9781118786352.wbieg0768.